



## MESTRADO INTEGRADO EM BIOENGENHARIA

# Biocompatibility assessment of Calcium Phosphate matrix reinforced with Carbon nanotubes

Gisela Fernanda dos Santos Ferreira

Dissertação submetida para obtenção do grau de  
**MESTRE EM BIOENGENHARIA – RAMO DE ENGENHARIA BIOMÉDICA**

---

**Orientadora:** Maria Ascensão Lopes  
(Professora Auxiliar do Departamento de Engenharia Metalúrgica e de Materiais da  
Faculdade de Engenharia da Universidade do Porto)

---



*To my parents, sister, grandparents and Hugo*



## Acknowledgements

Firstly, I would like to thank my supervisor Professor Ascensão Lopes for all the support, help, and availability. Thank you for being so nice. It was a nice pleasure to share these months with you.

Secondly I would like to thank everyone who contributes to the production of samples, Diogo Mata and Professor Rui Silva from Centro de Investigação em Materiais Cerâmicos e Compósitos (CICECO) at Universidade de Aveiro.

Thirdly I would like to express gratitude to Professor Maria Pia Ferraz and to technician Ricardo Silva from CEBIMED lab at Universidade Fernando Pessoa, for their help and kindness.

Then I must have to thank Engineer Ramiro Martins (Departamento de Engenharia Mecânica at Faculdade de Engenharia da Universidade do Porto) for his availability and clarifications on roughness measurements; Ricardo Vidal from Instituto de Engenharia Biomédica and Professor Fernão Magalhães from Departamento de Química of Faculdade de Engenharia da Universidade do Porto for the instructions of contact angle and zeta potential equipments. I have to express my gratitude to Professor Alice Vieira and to the post-doctoral student João Fernandes for their kindness and easy integration at Serviço de Bioquímica of Faculdade de Farmácia da Universidade do Porto.

Also, I am grateful to my class colleagues and friends for their company and friendship. I have o thank to all my Italian friends for being so nice and teaching me so many things. Furthermore, I am welcome to my parents, sister and Hugo which support me all the time and have had less time to spend with me. This work is for all of you!

Finally I would like to say “blood, sweat and tears”, “sangue suor e lágrimas”, “sangue, sudore e lacrime”, this is the slogan of my thesis. Only crying is missing... I hope to cry of happiness in the end!



## Abstract

Human lifespan has been increasing in the last decades, which contributes to the rising number of bone grafting procedures worldwide. Despite several biomaterials are available, none of them complies with all the requirements that an ideal bone graft should have.

Hydroxyapatite (HA), a calcium phosphate material with a composition closed to the inorganic part of bone, has been commercialized as a synthetic bone graft due to its biocompatibility, osteoconduction and osteointegration properties. However, it has low mechanical strength and cannot be used in the human body in load bearing sites.

Carbon nanotubes (CNTs) have become very popular in several applications due to its unique mechanical and electrical properties. Several attempts have been done regarding its use in the biomedical field. Since it is known that electrical stimulus has an important role in tissue regeneration, the use of CNTs in a bone graft is an interesting idea. The proposal of this thesis is therefore to characterize a calcium phosphate matrix reinforced with CNTs composite (CaP/CNTs). By the synergetic effect of individual properties of the materials, namely the biocompatibility of calcium phosphates and the unique mechanical and electrical properties of CNTs, this composite should present a high osteointegration.

The CaP/CNTs composite characterized in this thesis, supplied by Universidade de Aveiro, was developed by Diogo Mata, a PhD student from DECV-Universidade de Aveiro and has a superior electrical conductivity compared to its calcium phosphate matrix (CaP).

CaP/CNts composite was physicochemical characterized and biological evaluated. X-ray diffraction was used to characterize the chemical phase composition. Topography of samples for *in vitro* biological evaluation was observed by scanning electron microscopy, and surface roughness assessed by a profilometer. The level of carbon was analysed by combustion-InfraRed absorption. Wettability was assessed by the sessile drop method, and zeta potential evaluated by streaming potential measurements. Assessment of haemolytic properties of the materials was performed according to ASTM F756-00.

Regarding *in vitro* cell culture work, firstly an optimization of the electrical stimulation conditions were done applying AC current on MG63 cells and performing

MTT assays. Microbiological assays were performed to assure good laboratory practices during the application of electrical stimulus. Then, a primary cell culture with bone marrow cells was performed to evaluate the effect of electrical stimulus on osteoblasts grown on CaP/CNTs composite, an electrical conductive substrate. Subcutaneous screening tests for the composite in the granular form have also been started using an ovine model (ASTM F 1408-97 and ISO 10993-6).

CaP/CNTs composite was found to be composed by hydroxyapatite and  $\beta$ -tricalcium phases besides carbon; clumps of CNTs homogeneously distributed could be seen in the microstructure. The presence of CNTs led to a higher hydrophobicity and zeta potential of the composite compared to the CaP matrix ( $96.6^\circ$ ;  $61.5^\circ/-25.4\text{mV}$ ;  $-1.3\text{mV}$ , respectively), as expected. The haemolytic properties of tested granules of CaP/CNTs were unexpected found to be too high probably due to the general testing conditions proposed by the ASTM standard, which may not be adequate to materials with physical characteristics such as the one under evaluation.

The experiment with MG63 cells allowed achieving the optimum electrical stimulation conditions as 15 min of stimulus with AC current intensity of  $100\mu\text{A}$ . Primary cell culture studies showed similar proliferation patterns for CaP and CaP/CNTs materials, but the use of electrical stimulus promoted higher proliferation of cells grown on CaP/CNTs composite. These facts indicated that the inertness of carbon does not affect cell response but application of electrical stimulus in an electrical conductive substrate such as CaP/CNTs composite is highly positive for cell response.

With the work performed very interesting results were obtained for a novel composite material which combines the biocompatibility of a calcium phosphate matrix and the electrical conductivity of CNTs, and therefore have potential to be used in bone graft field.

**Keywords:** carbon nanotubes, calcium phosphate, bone regeneration.

## Resumo

A esperança média de vida no ser humano tem aumentado nas últimas décadas, o que contribui para o aumento de procedimentos de enxerto ósseo em todo o mundo. Apesar de existirem disponíveis no mercado diversos biomateriais, nenhum deles cumpre todos os requisitos que um enxerto ósseo ideal deve ter.

A hidroxiapatite (HA), um material de fosfato de cálcio com uma composição semelhante à parte inorgânica do osso, é comercializado como um enxerto ósseo sintético devido às suas propriedades de biocompatibilidade, osteocondução e osteointegração. No entanto, tem baixa resistência mecânica e não pode ser utilizado em locais de carga do corpo humano.

Os nanotubos de carbono (CNTs) tornaram-se muito populares em diversas aplicações, devido às suas propriedades mecânicas e eléctricas únicas. Na área biomédica têm sido feitas várias tentativas de aplicação. Desde que é sabido que o estímulo eléctrico tem um papel importante na regeneração dos tecidos, o uso de CNTs em enxertos ósseos é uma ideia interessante. O intuito desta tese é a caracterização de um compósito constituído por uma matriz de fosfato de cálcio reforçada com CNTs (CaP/CNTs). Este compósito deve apresentar uma alta osteointegração devido ao efeito sinérgico das propriedades individuais dos materiais que o constituem, ou seja a biocompatibilidade do fosfato de cálcio e as propriedades mecânicas e eléctricas únicas dos CNTs.

O compósito CaP / CNTs caracterizado nesta tese, fornecido pela Universidade de Aveiro, foi desenvolvido por Diogo Mata, um estudante de doutoramento do DECV-Universidade de Aveiro, e apresenta uma condutividade eléctrica superior quando comparada com a matriz de fosfato de cálcio (CaP).

O compósito CaP / CNTs foi caracterizado físico-quimicamente e avaliado biologicamente. Foi utilizada a difracção de raios-X para caracterizar a composição fásica. Foi observada, por microscopia electrónica de varrimento, a topografia de amostras para avaliação biológica *in vitro*, e a rugosidade da superfície foi avaliada por um profilometro. O nível de carbono foi analisado por combustão-absorção no infravermelho. A molhabilidade foi avaliada pelo método da gota séssil, e o potencial zeta avaliado pelo fluxo de potencial. A avaliação das propriedades hemolíticas dos materiais foi realizada de acordo com a norma ASTM F756-00.

No que diz respeito ao trabalho de cultura celular *in vitro*, em primeiro lugar foi efectuada uma optimização das condições de estimulação eléctrica, aplicando corrente alternada (AC) em células MG63 e realizando ensaios de MTT. Foram realizados ensaios microbiológicos para assegurar as boas práticas laboratoriais durante a aplicação do estímulo eléctrico. De seguida, foi realizada uma cultura de células primárias, com células da medula óssea, para avaliar o efeito do estímulo eléctrico sobre os osteoblastos cultivados no compósito CaP / CNTs, uma superfície condutora eléctrica. Foi também iniciado um teste subcutâneo preliminar com implantação de grânulos do compósito, utilizando um modelo ovino (ASTM F 1408-97 e ISO 10993-6).

O compósito CaP/CNTs é composto por hidroxiapatite e  $\beta$ - fosfato de tricálcio para além de carbono; a microestrutura apresenta agregados de CNTs distribuídos de forma homogénea. A presença de CNTs contribui para uma maior hidrofobicidade e potencial zeta do compósito em comparação com a matriz de hidroxiapatite ( $96.6^\circ$ ;  $61.5^\circ$  /  $-25.4\text{mV}$ ;  $-1.3\text{mV}$ , respectivamente), como esperado. As propriedades hemolíticas dos grânulos testados CaP/CNTs revelaram-se demasiado elevadas, provavelmente devido a condicionamentos do protocolo proposto pela norma ASTM, que pode não ser o mais adequado para um material com as propriedades físicas como o material em estudo.

As experiências com células MG63 permitiram definir condições óptimas de estimulação eléctrica como sendo 15 min de estímulos com corrente alternada de  $100\mu\text{A}$ . Os estudos com culturas de células primárias mostraram um padrão de proliferação similar entre os materiais CaP e CaP/CNTs, contudo o uso de estimulação eléctrica promoveu uma maior proliferação das células cultivadas no compósito CaP/CNTs. Estes resultados indicam que a inércia do carbono não afecta a resposta celular, contudo a aplicação de estímulos eléctricos num material condutor eléctrico como o compósito CaP/CNTs é altamente benéfico para a resposta celular.

Os resultados obtidos com o desenvolvimento deste trabalho são muito promissores quanto ao potencial deste novo material compósito para aplicação na área dos implantes ósseos, uma vez que combina a biocompatibilidade de uma matriz de fosfato de cálcio com a condutividade eléctrica dos nanotubos de carbono.

**Palavras-chave:** nanotubos de carbono, fosfato de cálcio, regeneração óssea.

## Riassunto

Negli ultimi decenni l'aspettativa di vita è aumentata, e ciò ha contribuito al crescente numero di procedure di innesto osseo in tutto il mondo. Nonostante per tali applicazioni siano disponibili diversi biomateriali, nessuno di essi è in grado di soddisfare tutti i requisiti che un innesto osseo ideale dovrebbe avere.

L'idrossiapatite (HA), un materiale a base di fosfato di calcio con una composizione simile alla parte inorganica delle ossa, è stato commercializzato come un innesto osseo sintetico per le sue proprietà di biocompatibilità, osteoconduttiva e osteointegrazione. Tuttavia, ha una bassa resistenza meccanica e non può essere utilizzati nel corpo umano nei siti maggiore portanza.

I nanotubi di carbonio (CNTs) sono diventati molto popolari in diverse applicazioni grazie alle loro proprietà meccaniche ed elettriche. Molti tentativi sono stati fatti per quanto riguarda il loro utilizzo in campo biomedico. Poiché è noto che lo stimolo elettrico ha un ruolo importante nella rigenerazione dei tessuti, l'utilizzo di CNTs in un innesto osseo rappresenta un'idea interessante e innovativa. La scopo di questa tesi è quindi la caratterizzazione di un composito di una matrice di idrossiapatite rinforzata con CNTs (CaP / CNTs). Per effetto sinergico delle singole proprietà dei materiali, cioè la biocompatibilità di idrossiapatite e le proprietà uniche meccaniche ed elettriche di CNTs, questo composito dovrebbe presentare un alto grado di osteointegrazione.

Il CaP / CNTs composito caratterizzato in questa tesi, forniti da Universidade de Aveiro, è stato sviluppato da Diogo Mata, uno studente di dottorato presso DECV-Universidade de Aveiro e ha una conducibilità elettrica superiore rispetto alla sua matrice di fosfato di calcio (CaP).

CaP / CNTs composito è stato caratterizzato dal punto di vista fisico.chimico e valutato per quanto riguarda le sue proprietà biologiche. Per caratterizzare la composizione delle fasi chimiche è stato utilizzato il principio della diffrazione dei raggi X. Successivamente è stata osservata la topografia dei campioni per la valutazione biologica *in vitro* mediante microscopia elettronica a scansione, mentre la rugosità superficiale è stata valutata da un profilometro. Il livello di carbonio è stato analizzato mediante test di combustione-assorbimento nell'infrarosso. La bagnabilità è stata valutata mediante il metodo goccia sessile, e il potenziale zeta valutato da misure di potenziale di flusso. La valutazione delle proprietà emolitiche dei materiali è stata effettuata secondo la norma ASTM F756-00.

Per quanto riguarda il lavoro di colture cellulari *in vitro*, in primo luogo è stata realizzata una ottimizzazione delle condizioni di stimolazione elettrica, mediante l'applicazione di una corrente alternata (AC) su cellule MG63 e dall'esecuzione di test MTT. Analisi microbiologiche sono state poi effettuate per assicurare buone pratiche di laboratorio durante l'applicazione dello stimolo elettrico. Successivamente è stata eseguita una coltura cellulare primaria con cellule del midollo osseo, per valutare l'effetto di stimolo elettrico sugli osteoblasti coltivati su CaP / CNTs composito, un substrato conduttivo elettrico. Infine sono stati iniziati anche test di screening per via sottocutanea per il composito in forma granulare utilizzando un modello di ovini (ASTM F 1408-97 e ISO 10993-6).

Il composito CaP /CNTs è composto da idrossiapatite e  $\beta$ -fosfato tricalcico, oltre a carbonio; la microstruttura presenta aggregati di CNT omogeneamente distribuiti. La presenza di nanotubi di carbonio contribuisce ad una maggiore idrofobicità e ad un potenziale zeta del composito più elevato rispetto alla matrice di idrossiapatite ( $96.6^\circ$ ,  $61.5^\circ/-25.4\text{mV}$ ,  $-1.3\text{mV}$ , rispettivamente), come previsto. Le proprietà emolitiche dei granuli testati CaP / CNTs erano invece troppo alte, probabilmente a causa dei vincoli del protocollo proposto da ASTM, che non può essere il più appropriato per un materiale con proprietà fisiche che lo caratterizzano.

Gli esperimenti con cellule MG63 hanno permesso di definire le condizioni ottimali di stimolazione elettrica di 15 minuti di stimolazione con corrente alternata di  $100\mu\text{A}$ . Studi con colture cellulari primarie hanno mostrato un andamento simile della proliferazione di materiali CaP e CaP/CNTs ,tuttavia l'uso di stimolazione elettrica ha promosso una maggiore proliferazione di cellule coltivate in composito CaP/ CNTs. Questi risultati indicano che l'inerzia del carbonio non influisce sulla risposta cellulare, tuttavia l'applicazione della stimolazione elettrica in un materiale elettricamente conduttivo come il composito CaP/CNTs è di grande beneficio per la risposta cellulare.

I risultati ottenuti da questo lavoro sono molto ottimistici circa il potenziale di questo nuovo materiale composito per l'impiego nelle zone soggette ad impianti ossei, poiché combina la biocompatibilità di una matrice di fosfato di calcio con la conducibilità elettrica dei nanotubi di carbonio.

**Parole-chiave:** nanotubi di carbonio, fosfato di calcio, innesto osseo.





# Contents

<i>Acknowledgements</i> .....	v
<i>Abstract</i> .....	vii
<i>Resumo</i> .....	ix
<i>Riassunto</i> .....	xi
<i>List of figures</i> .....	xix
<i>List of tables</i> .....	xxi
<i>Abbreviations</i> .....	xxiii
<b>1      Introduction and Aims</b> .....	<b>1</b>
<b>2      Context</b> .....	<b>3</b>
<b>2.1      Bone Considerations</b> .....	<b>3</b>
2.1.1      Functions .....	3
2.1.2      Composition.....	3
2.1.3      Remodeling process.....	3
2.1.4      Promoting factors of bone growth .....	4
<b>2.2      Bone substitutes</b> .....	<b>6</b>
2.2.1      Natural versus Synthetic .....	6
<b>2.2.1.1      Synthetic ceramic materials</b> .....	<b>7</b>
2.2.1.1.1      Bioactive glass.....	7
2.2.1.1.2      Calcium phosphate based materials.....	7
<b>2.3      Carbon Nanotubes</b> .....	<b>8</b>
2.3.1      Advantages and constraints .....	10
2.3.2      Carbon Nanotubes for bone regeneration .....	10
<b>3      Materials and Methods</b> .....	<b>14</b>
<b>3.1      Physicochemical Characterization</b> .....	<b>14</b>
3.1.1      X-Ray Diffraction .....	15
3.1.2      Roughness.....	15

3.1.3	Carbon analysis by Infrared absorption .....	16
3.1.4	Wettability .....	16
3.1.5	Zeta Potential.....	17
3.1.6	Scanning Electron Microscopy .....	14
<b>3.2</b>	<b>Biological Evaluation .....</b>	<b>19</b>
3.2.1	<i>In vitro</i> conditions.....	19
3.2.1.1	Blood compatibility.....	19
3.2.1.2	Optimization of the electrical stimulation conditions.....	20
3.2.1.2.1	Cell Culture .....	21
3.2.1.2.2	Cell Proliferation .....	21
3.2.1.2.3	Statistical Analysis .....	23
3.2.1.3	Dye Interaction with materials .....	23
3.2.1.4	Microbiological assays .....	24
3.2.1.4.1	Gram Staining.....	25
3.2.1.4.2	Catalase test.....	26
3.2.1.4.3	Oxidase test .....	26
3.2.1.5	Primary Cell culture .....	27
3.2.1.5.1	Cell proliferation .....	27
3.2.1.5.2	Statistical Analysis .....	28
3.2.1.5.3	Flow cytometry – cell fixation .....	28
3.2.1.5.4	Scanning Electron Microscopy.....	28
3.2.2	<i>In vivo</i> Conditions.....	29
3.2.2.1	Preliminary subcutaneous screening test.....	29
<b>4</b>	<b>Results and General Discussion .....</b>	<b>31</b>
<b>4.1</b>	<b>Physicochemical Characterization .....</b>	<b>31</b>
4.1.1	X-Ray Diffraction .....	32
4.1.2	Roughness.....	33
4.1.3	Carbon analysis by Infrared absorption .....	34
4.1.4	Wettability .....	35

4.1.5	Zeta Potential .....	35
4.1.6	Scanning Electron Microscopy .....	31
<b>4.2</b>	<b>Biological Evaluation .....</b>	<b>36</b>
4.2.1	<i>In vitro</i> conditions .....	36
4.2.1.1	Hemolytic Properties.....	36
4.2.1.2	Optimization of the electrical stimulation conditions.....	39
4.2.1.1	Dye-Interaction with materials .....	42
4.2.1.2	Microbiological assays.....	43
4.2.1.3	Primary cell culture .....	45
4.2.2	<i>In vivo</i> conditions.....	48
<b>5</b>	<b>Concluding remarks and future work .....</b>	<b>49</b>
<b>5.1</b>	<b>Conclusions.....</b>	<b>49</b>
<b>5.2</b>	<b>Future Work.....</b>	<b>49</b>
<b>References .....</b>		<b>51</b>



## List of figures

<i>Figure 1- Comparison of human survivability in year 1900 versus 2000 with effects of age on the quality of connective tissue (2).</i> .....	1
<i>Figure 2 – Bone remodelling process: resorption of the old bone by osteoclasts and new formation by osteoblasts; the cells trapped in the matrix are denominated osteocytes (10).</i> .....	4
<i>Figure 3 - Molecular structure of SWCNT (left) and MWCNT (right) (67); permission authorized.</i> .....	9
<i>Figure 4 – Scanning scheme of roughness measurements for each sample.</i> .....	16
<i>Figure 5 - OCA 15 Optical Contact Angle System (Data Physics, detail of the thermostatted stainless-steel chamber with two pools of water, syringe and illumination.</i> .....	17
<i>Figure 6 – Scheme with drops order during the experiment.</i> .....	17
<i>Figure 7 – Stamp cell used with CaP/CNTs samples attached with double-side adhesive tape.</i> .....	18
<i>Figure 8 – Equilibrium of ions between solid and liquid phases.</i> .....	18
<i>Figure 9 - a) Venipuncture and collection of blood to citrate tubes, b) tubes to each type of blood: negative control, positive control, CaP and CaP/CNTs.</i> .....	20
<i>Figure 10 – a) Current flow of cell culture stimulation, b) agar-KCl bridges soaked in KCl solution..</i> .....	21
<i>Figure 11 – Electrical Stimulation device.</i> .....	23
<i>Figure 12 – Stimulation apparatus a) outside the cabinet flow, b) inside the cabinet flow.</i> .....	25
<i>Figure 13 – Gram staining step: a) fixation on fire, b) laminas already fixed, c) addition of violet crystal, d) Lugol solute, e) safranine.</i> .....	26
<i>Figure 14 – a) Animal washed, shaved and disinfected in dorsal area, b) Performing the subcutaneous space to implant the open tubes with granules, c) Animal sutured in the end of the intervention.</i> .....	30
<i>Figure 15 - SEM micrographs of a) CaP and b) CaP/CNTs samples (1000x).</i> .....	31
<i>Figure 16 - SEM micrographs of a) CaP and b) CaP/CNTs samples (20000x).</i> .....	31
<i>Figure 17 - XRD patterns of CaP and CaP/CNTs materials.</i> .....	32
<i>Figure 18 – XRD patterns of CaP and CaP/CNTs materials.</i> .....	33
<i>Figure 19 – CaP tablets after sintering process.</i> .....	34
<i>Figure 20 – Percentage of haemolysis of each material: nitrile (positive control), CaP and CaP/CNTs. The haemolysis found on blood (negative control) was subtracted to all the conditions (normal haemolysis).</i> .....	37
<i>Figure 21 – Optical microscopy pictures of a) blood – negative control, b) blood with nitrile - positive control, c) blood in contact with CaP, d) blood in contact with CaP/CNTs. All the samples have a dilution of 1:10 and an augmentation of 1000x (oculars + objectives).</i> .....	38

<i>Figure 22 – Optical microscopy images; a) CaP granules of 250 µm to 500µm, b) CaP/CNTs granules of 250µm to 500µm. (Augmentation of 100x (objectives +oculars). .....</i>	39
<i>Figure 23 – Effects of 10µA and 100µA electrical stimulus and application time (15,30 and 60min) on the growth of MG63 cells. MG63 cells were grown on two replicates of plastic culture dishes of 58cm<sup>2</sup>. MTT assay was carried out and the absorbance was read at 545nm. The bars show the averaged of two separate experiments ± SD (vertical lines). *: Statistically different from the control (P≤0.05). .....</i>	40
<i>Figure 24 - Effects of 100µA and 200µA of electrical stimulus and application time (15 and 15+15min) on the growth of MG63 cells. MG63 cells were grown on two replicates of plastic culture dishes of 58cm<sup>2</sup>. MTT assay was carried out and the absorbance was read at 545nm. The bars show the averaged of two separate experiments ± SD (vertical lines). *: Statistically different from the control (P≤0.05).....</i>	41
<i>Figure 25 – MTT interaction with a) CaP samples, b) CaP/CNTs samples.....</i>	42
<i>Figure 26 – ALP interaction with a) CaP samples, b) CaP/CNTs samples. ....</i>	43
<i>Figure 27 – Cell proliferation of human bone marrow cells grown on polystyrene treated plates, CaP and CaP/CNT samples with and without stimulation for 28 days. *: Statistically different from the control, + statistically different from the CaP, # statistically different from the CaP/CNT (P≤0.05)...</i>	46
<i>Figure 28 – Scanning electron microscopy micrographs a) spread cells on CaP/CNTs samples on 3<sup>rd</sup> day, b) 10<sup>th</sup> culture day on CaP surface, c) Damaged cells on CaP samples after 7days of culturing. .</i>	48

## List of tables

<i>Table 1 - Current and time conditions tested with MG-63 cells .....</i>	22
<i>Table 2 - Surface roughness (Ra) values for CaP and CaP reinforced with CNTs. ....</i>	33
<i>Table 3 – Percentage (%) of carbon found by infrared absorption on CaP and CaP/CNTs samples....</i>	34
<i>Table 4 - Contact Angles of water on CaP and CaP/CNTs samples (<math>\theta</math>).....</i>	35
<i>Table 5 - Zeta potential values for CaP and CaP reinforced with CNTs (mV). ....</i>	36
<i>Table 6 – Hemolytic grade according to standard ASTM F756.....</i>	37
<i>Table 7 – Microbiological growth in BHI plates.....</i>	44
<i>Table 8 - Microbiological assays of organism's growth. ....</i>	45



## Abbreviations

<b>Ar</b>	Argon
<b>ALP</b>	Alkaline phosphatase
<b>ANOVA</b>	Analysis Of Variance
<b>ASTM</b>	American Society for Testing and Materials
<b>BHI</b>	Brain Heart Infusion
<b>CaP</b>	Calcium Phosphate
<b>CICECO</b>	Centro de Investigação em materiais Cerâmicos e Compósitos
<b>CMF</b>	Combined Magnetic Field
<b>CNTs</b>	Carbon NanoTubes
<b>DCES</b>	Direct Current Electrical Stimulation
<b>DCEV</b>	Departamento de Engenharia de Cerâmica e do Vidro
<b>DMSO</b>	Dimethyl Sulfoxide
<b>EDS</b>	Energy-Dispersive Spectroscopy
<b>EKA</b>	Electro Kinetic Analyzer
<b>FCS</b>	Fetal Calf Serum
<b>FEUP</b>	Faculdade de Engenharia da Universidade do Porto
<b>FTIR</b>	Fourier Transform Infra Red (spectroscopy)
<b>HA</b>	HydroxyApatite
<b>ISO</b>	International Organization for Standardization
<b>KCl</b>	Potassium Chloride
<b>NaOH</b>	Sodium Hydroxide
<b>MWCNTs</b>	Multi-Walled Carbon NanoTubes
<b>MTT</b>	MethylThiazolyldiphenyl-Tetrazolium bromide
<b>PBS</b>	Phosphate Buffered Saline solution

<b>PEMF</b>	Pulsed ElectroMagnetic Field
<b>SBF</b>	Simulated Body Fluid
<b>SDS</b>	Sodium Dodecyl Sulphate
<b>SEM</b>	Scanning Electron Microscopy
<b>SPS</b>	Spark Plasma Sintering
<b>SWCNTs</b>	Single-Walled Carbon NanoTubes
<b>TCP</b>	Tri-Calcium Phosphate
<b>TCPS</b>	Tissue Culture plates of PolyStyrene
<b>Ti</b>	Titanium
<b>UHMWP</b>	Ultra High Molecular Weight Polyethylene
<b>XRD</b>	X-Ray Diffraction
<b>ZP</b>	Zeta Potential
<b><math>\alpha</math>-MEM</b>	A-Minimum Essential Medium

# 1 Introduction and Aims

Since ever people try to apply medical knowledge to improve human lives in order to reduce suffer and earlier death. With technology development, the typical art of medicine was improved, providing a wide range of effective diagnostic and therapeutic treatments (1). Due to these advances, life expectancy is much higher now than one century ago (nowadays is around 80 years meanwhile in the beginning of 20<sup>th</sup> century was roughly 50 years). Then, human body is currently exposed to higher cumulative stress, which results in tissue damaging (figure 1), so new therapies should be developed to meet this average life expectancy growing (2).

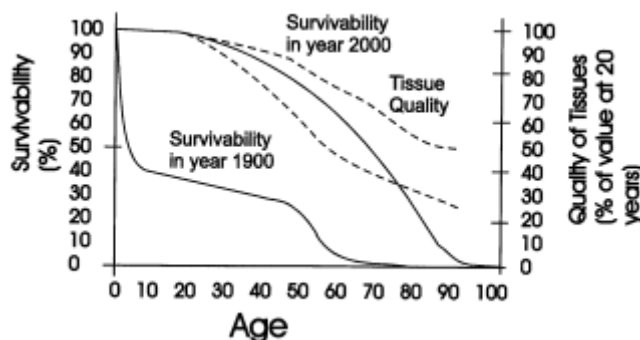


Figure 1- Comparison of human survivability in year 1900 versus 2000 with effects of age on the quality of connective tissue (2).

Bone grafts field has a high impact on life quality in the new century, and has also a lot to develop to fulfil the new challenges (3).

The most clinically used graft materials are calcium phosphate based due to its biocompatibility, despite not being an ideal graft. Besides the electrical activity observed in bone is somehow the mediator of its remarkable repair and therefore an electrical stimulus alone can stimulate the bone healing. In fact, electrical stimulation therapies have been used for more than 30 years to enhance spinal fusions and in ununited fractures (4). The material used in this thesis is a calcium phosphate matrix reinforced with carbon nanotubes (CNTs) developed by Diogo Mata, a PhD student from DECV-Universidade de Aveiro; this composite material (CaP/CNTs) was developed to have a higher electrical conductivity than calcium phosphate materials.

This thesis begins with an overview of literature (Chapter 2) on bone physiology, bone grafts, carbon nanotubes (CNTs) and their potential use in biomedical field.

Chapter 3 provides the methods used to physicochemical characterize the calcium phosphate matrix reinforced with CNTs (CaP/CNts), and describes the biological evaluation performed.

In Chapter 4 results are presented and discussed.

Chapter 5 present general conclusions and suggestions for future work to complete the study of the CaP/CNTs composite used in this thesis.

The author of this thesis performed all the experimental work described in this thesis except the analysis of carbon level and X-Ray diffraction Analysis. The animal experimentation was performed by vets but with active participation of the author.

## 2 Context

### 2.1 Bone Considerations

#### 2.1.1 Functions

The skeleton provides the internal support system to humans and all the vertebrates. There are two different types of bone such as flat and long bones, depending on their functions. They have a number of roles as supporting all the weight and insertion of the several muscles, protection of vital organs (brain and abdominal organs) and bone marrow, and as a store of minerals particularly calcium and phosphate (5). Bones are also crucial on movement of the body and on producing blood cells (1).

#### 2.1.2 Composition

Bone is constituted by two different phases: organic and mineral, containing cells and vessels. The organic compounds are essentially type I collagen (about 90%), and some glycoproteins and proteoglicans as osteocalcin, osteopontin, etc. Collagen type I organizes itself in fibrils, and then in parallel assays with gaps to join together minerals. Fibrils are established by inter and intra-crosslinks which will provide the mineralization (6, 7). The inorganic part is created when the organic compounds are calcified with the deposition of crystals of highly substituted hydroxyapatite,  $\text{Ca}_{10}(\text{PO}_4)_6(\text{OH})_2$ , with a calcium phosphate ratio of 5:3 (1.67) (8, 9).

#### 2.1.3 Remodeling process

Bone is a living organ in constant remodeling process and calcium availability in the body (1). There are three main types of cells: osteoclasts, osteoblasts and osteocytes. Osteoclasts are responsible for the resorption of old bone, meanwhile osteoblasts produce new bone – figure 2. These cells have the main role in the remodeling process, crucial to the bone integrity and mineral homeostasis. When

osteoblasts, producing new bone, have been trapped into the extracellular matrix are called osteocytes. When the bone is produced (immature) and has a random organization it is called woven bone. Accordingly, this type of bone is gradually replaced by definitive bone named lamellar, which is organized (successive layers of collagen fibers, with different directions). Depending on the part of the bone, lamellar production could be different. In the external parts of the bone, is formed a thick and dense layer – cortical bone (about 80-90% of calcification), whereas internal space of the bones is filled with a network of thin calcified trabeculae – trabecular bone (about 15-25% of calcification) – the space between trabeculae is filled with bone marrow (5).

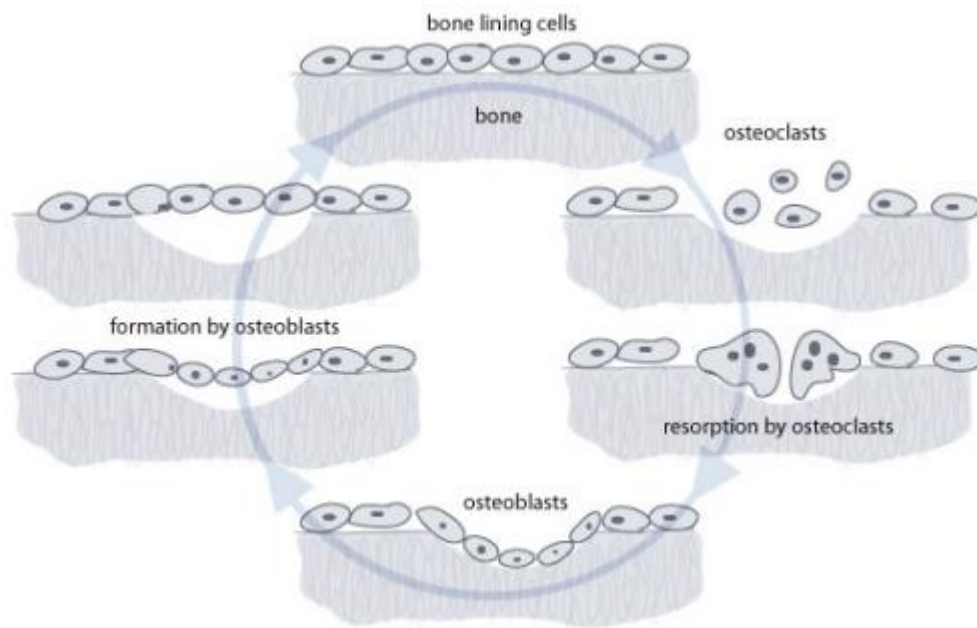


Figure 2 – Bone remodelling process: resorption of the old bone by osteoclasts and new formation by osteoblasts; the cells trapped in the matrix are denominated osteocytes (10).

## 2.1.4 Promoting factors of bone growth

There are several factors that can compromise bone growing as nutrition, hormones, electrical stimulation and physical stress.

Nutrition is very important in this topic because it will provide molecules which are co-inducers of some processes. For example vitamin C is necessary to collagen

production by osteoblasts, and vitamin D is useful to calcium absorption on digestive tube (and then to bone calcification) (11).

Hormones also have importance because they stimulate tissues growth in general. Specifically thyroid and sexual hormones are responsible for the pace of growth (11).

Physical stress can increase bone formation. It is processed when muscles contract and pull their attachments, resulting on stress stimulation. The effects of mechanical load depend on magnitude, duration and rate of applied load, and it should be cyclic to an effective stimulation. Mechanosensory apparatus and mechanochemical pathways are turned on when the load is applicable and only after 3-5 days the bone formation is visualized (12-14).

Luigi Galvini in 1792 documented the human and animal's ability to generate endogenous electric signals (15). This is visualized when a tissue is damaged and injury potentials create electric fields which will stimulate wound healing (16). Several publications have reported that mechanical modifications alter endogenous electrical signals.

Studies with human femur and tibia bones demonstrated frequency dependency of bone regeneration. Between 10Hz and 10KHz, conductivity and phase angle increase with frequency and then is constant to higher frequencies. With the specific impedance the values diminished until  $10^3$ Hz and then remain constant (17).

Electrical stimulation has been demonstrated effectiveness on bone growth stimulation, as *in vitro*, *in vivo* and in clinical applications (4, 18-24). There are different processes of stimulation: direct current electrical stimulation (DCES), pulsed electromagnetic fields (PEMF), and combined magnetic fields (CMF). It was found that DCES presents better results than CMF, which in turn has better results than PEMF in wound healing and correction of bone defects (4). Also, the frequency stimulation has a range of 10Hz to 100Hz (18, 21, 22, 24). Electrical stimulation devices are already commercialized by several companies (25, 26).

## 2.2 Bone substitutes

Bone grafts have been widely used in surgical procedures to stimulate bone healing, filling defects following removal of bone tumours or other bone diseases, spinal fusions, and in dentistry (9, 27-32). Bone grafting is one of the most used transplantations, where 2.2 million people worldwide are exposed to these procedures. For this reason, research still ongoing trying to challenge the future. This improvement could provide a better life quality to a higher life expectancy society(28).

There are three crucial characteristics to bone regeneration. To a final osteointegration (surface bonding between the host bone and the grafting material), the material should have the ability to osteogenesis, osteoinduction and osteoconduction. Osteogenesis provides stem cells with osteogenic potential, or factors that promote proliferation and differentiation into osteoblasts. Then, osteoinduction is the capability to stimulate or activate the host mesenchymal stem cells from the surrounding tissues to differentiate into osteogenic cells (this is mediated by a cascade of signals and activation of extra and intracellular receptors). On the other hand, osteoconduction provides a passive porous scaffold to support or direct bone formation. It is characterized by the process of invasion and growth of blood-vessels, and migration of stem cells from local sites to bone graft (28, 33).

### 2.2.1 Natural versus Synthetic

Natural and synthetic substitutes differ on their origin. However, there are some other differences which are crucial to their evolution in the market, mainly, availability amount and possible immunological response.

Natural substitutes include the *gold standard* of bone grafts – autografts (28). This is mainly because of their minimum immunological rejection (except for contamination at harvest), complete histocompatibility and provide the best osteoconductive (mineral matrix), osteogenic (stem cells, proteins, cartilage) and osteoinductive (proteins) properties, once it is a part of the host.

A bone allograft is bone harvested from other people, usually from cadaver. In this case the disadvantages are related with lack of histocompatibility, immunogenic

and infectious problems (30, 34). Xenografts represent the use of bone from other species to grafting such as bovine animals. Porcine xenografts are widely used to temporary coverage of clean wounds (9). They cannot have lipids, proteins and antigens from the donor to avoid contamination and immunologic responses (34).

Corals, proteins as collagen, and polysaccharides as chitosan are also natural bone grafts already studied. It has been studied the association between these natural bone grafts and calcium phosphates showing biocompatibility and osteoconduction. Some of these associations are already applied on medical procedures as Healos® (collagen combined with hydroxyapatite) (34-37).

In order to find the ideal properties that promote bone regeneration and to overcome the problem of quantity availability, researchers have been developing synthetic materials, by proposing easier and cheaper methods (9, 28, 33). Examples of synthetic biomaterials are ceramics (as hydroxyapatite, TCP) and polymers (as poly(glycolic acid), poly( $\epsilon$ -Caprolactone)).

## **2.2.1.1 Synthetic ceramic materials**

### **2.2.1.1.1 Bioactive glass**

Bioactive glass ceramics were developed at first by Hench. He demonstrated the capacity to bond to bone in a quick and hard way by an apatite layer (34). In some studies with rats, it was found bioglass biocompatibility (absence of adverse cellular reactions); on rabbit studies, filler effect was greater with bioactive glass than with autogenous bone, and glass fiber scaffolds are completely resorbed after 6 months. Though this favourable characteristics depend on the glass composition (30).

### **2.2.1.1.2 Calcium phosphate based materials**

Calcium phosphates are widely used as cement (adding an aqueous solution) improving the ability to custom-fill defects and increased compressive strength. Although they present some disadvantages such as brittleness and having little tensile strength, which decreases structural resistance. For these reasons it is not generally used by itself in sites under load (27, 38). To have a porosity which allows osseous

ingrowth (minimum of 100 µm, and 300µm - 500 µm as ideal), the material should be processed and sintered under specific conditions (27, 34).

Synthetic hydroxyapatite (HA)  $\text{Ca}_{10}(\text{PO}_4)_6(\text{OH})_2$ , is similar to natural hydroxyapatite in human bone, with a calcium-to-phosphate atomic ratio of 1.67. It presents low resorption and bone remodelling. Also, due to their suitable structure to osteointegration, HA has been widely used (30). Synthetic hydroxyapatite is normally produced with other calcium phosphates aiming to improve biological and mechanical properties (39-41). In clinical cases where it is used in a granular form, some difficulties to maintain the granules in the intervention area can arise. In these cases it is normally used associated with gel based materials to help the stabilization such as collagen ((34, 37), poly (ethylene glycol) (42-44), chitosan (45-48), or alginate (49-53).

Tri-calcium phosphate is a biocompatible bio absorbable calcium phosphate. The chemical composition and crystallinity of the material are similar to those of the mineral phase of bone. The nominal composition of TCP is  $\text{Ca}_3(\text{PO}_4)_2$ . It exists in either  $\alpha$  or  $\beta$ -crystalline forms (30), with different levels of degradation. The biodegradation is faster when compared to HA, and it may represent a disadvantage because implies a quick loss of structure support (34).

Ceramic materials have a lot of good characteristics to bone grafting but they should be used in combination to challenge the disadvantages of each one individually. Biocomposites have becoming more important on bone remodelling and homogeneous dispersions of  $\alpha$ - and  $\beta$ -TCP phases in an HA matrix have been performed. These biomaterials show better biocompatible and better mechanical properties than pure phase HA (34, 39-41).

## 2.3 Carbon Nanotubes

In 1991 were discovered multi-walled carbon nanotubes , and in 1993 single-walled analogous (54). Carbon nanotubes (CNTs) are the material lying between fullerenes and graphite as a new member of carbon allotropes with a cylindrical nanostructure. Each carbon nanotube (CNT) is characterized by its diameter and chiral angles, which perform different properties to different applications (55, 56).

In general, CNTs are classified as either single-walled carbon nanotubes (SWCNTs) with diameters typical range between 0.8 and 2 nm, which are much more difficult to manipulate accurately by the conventional patterning technology, or multi-walled carbon nanotubes (MWCNTs) (a concentric arrangement of numerous cylinders reaching diameters of up to 100 nm) – figure 3, even though there are more types reported (57, 58).

Carbon nanotubes (CNTs) have a unique geometry and extraordinary mechanical, electrical and thermal conductivity properties (59-62). These single properties could be used as reinforcement or additives in several materials to improve their properties and introduce novel functionalities in several areas, such as electronic, energy, mechanical, sensors, emission and lighting, and biological fields as medicine and nanotechnology (57) (63).

Nowadays, there are three methods of producing CNTs: arc discharge, laser ablation and chemical vapour deposition. After that some procedures should be taken such as purification methods (important to avoid structural damage of the CNTs produced) and functionalization. This process modifies the chemical surface of CNTs in order to interact with other materials once they have a cylindrical form (figure 3), and chemical inertness and low surface energy of the graphitic structure which could be problematic to a correct dispersion into different materials (64-66).

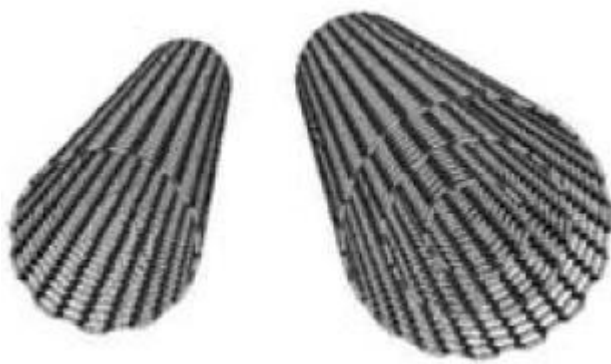


Figure 3 - Molecular structure of SWCNT (left) and MWCNT (right) (67); permission authorized.

The functionalization of CNT can be performed either at the side-walls or at the oxidatively opened-tips. Functionalization can be either through covalent attachment of organic units or *via* supramolecular means.

### 2.3.1 Advantages and constraints

Conductive polymers have many advantages over metallic conductors (68); although carbon nanotubes have much more advantages when compared to conducting polymers such as stability, mechanical strength and flexibility (55).

It has been studied the use of carbon nanotubes in preservation of cells, and giving strength and flexibility to scaffolding in order to promote integration with the host tissue. They can be incorporated in other materials to reinforce the scaffolds; also can provide electrical conductivity to these materials (important in directing cell growth). CNTs have the property of adhesiveness and absorbency, this can be used on drug or gene delivery (57).

The safety of CNTs has not been yet confirmed, there are some studies about inhalation, and some others about implantation, but without definitely conclusions. There are favourable and non-favourable results (67, 69, 70). The effects of length and diameter of CNTs, and which is the most suitable chemical functionalization still not clearly defined (57, 59, 71).

### 2.3.2 Carbon Nanotubes for bone regeneration

Some research works have been published regarding the use of CNTs in biomaterials for bone regeneration. Several attempts have been made by associating CNTs with some polymers to provide better mechanical properties and electrical conductivity.

Zawadzak *et al* studied, *in vitro*, the potential of a composite made of polyurethane foams with CNT coating to bone tissue engineering due to their high interconnected porosity, bioactivity and nanostructured surface topography (72). Nanocomposites of CNTs with poly(lactic acid) were assessed *in vitro* cultures electrically stimulated (73-75). Also the combination with other polymers has been reported: testing *in vitro* with MG63 cells in MWCNTs/UHMWP (ultra molecular weight polyethylene) composites (76), polyurethane scaffolds coated with CNTs assessed by simulated body fluid (SBF) (77), poly(propylene fumarate) composite was evaluated in a rabbit model (78).

In the field of ceramics, as the inorganic part of bone is composed of a calcium phosphate, the association of hydroxyapatite with CNTs has led to many publications. Most of them are focused on processing methods, whereas a few are dedicated to *in vitro* and *in vivo* biological assessment of the new materials.

*Aryal et al* described a method to synthesize HA using carbon nanotubes matrix. They purchased MWCNTs and removed the amorphous carbon particles by washing with concentrated hydrochloric acid and nitric acid. MWCNTs were functionalized with carboxylic groups. They used those carbon nanotubes to react with an aqueous solution of calcium chloride, and after 1hour de HA was precipitated. They found by FTIR and XRD that the HA produced was close to the natural one (79).

*Tan et al* worked on a nanohybrid made of hydroxyapatite and multi-walled carbon nanotubes. Firstly, carbon nanotubes were functionalized with surfactant sodium dodecyl sulfate (SDS). Secondly, with six cycles of aqueous solutions of  $\text{CaCl}_2$  and  $\text{Na}_2\text{HPO}_4$ , biomineralization was completed. By FTIR and XRD analysis it was confirmed that the mineral was HA, proving the usability of the process to create this composite (80).

A slurry of HA was mixed with MWCNTs using Hybrid Defoaming Mixer for 1 hour. Dried slurry was sintered by using spark plasma sintering at 5-120MPa pressure, 1200-1250 °C and in vacuum or  $\text{N}_2$  atmosphere. By XRD analysis it was shown the presence of HA and MWCNTs. This kind of production contributed to increase the fracture toughness (81).

*Li et al* compared the MWCNTs/HA composites made by two different processes. They produced HA by the typical method of precipitation, and bought multi-wall carbon nanotubes. By ultrasonic vibration HA and CNTs were dispersed during 1h; then water was removed, and a powder was obtained. This composite powder was made stable by cold press molding and cold isostatic compaction. After that, sintering processes used were pressureless sintering in vacuum and pressureless sintering in Ar. It was proved that both type of composites have bending strength and fracture toughness better than pure HA. Composite sintered in vacuum has much higher mechanical properties (strong interface junction and less pores) than the one sintered in Ar. Comparing two different composites MWCTNSs/HA and  $\text{ZrO}_2/\text{HA}$  *in*

*vivo*, they found no toxicity or inflammatory reaction in the tissue around (2weeks), and better histocompatibility on MWCNTs/HA composite (82).

Xu, Khor, Sui and Chen presented a new HA/CNTs composite. The authors purchased commercially multiwalled carbon nanotubes. It was used a low amount of CNT powder (2 vol.%) to mix with 98 vol.% spray dried HA powder in ethanol and mechanical stirred for 5 days. The dispersed mixture was then dehydrated in an open air. A spark plasma sintering (SPS) system was used to consolidate the obtained powder feedstock at various sintering temperatures. A pressure of 7.5 MPa was initially applied. The results showed that the use of spark plasma sintering lead to a high value of modulus (~131.1 GPa) and hardness (~6.86 GPa) of CNT reinforced HA at the sintering temperature of 1100°C. In addition, the study has further clarified that the presence of CNTs in HA has promoted growth and adhesion of osteoblast cells at the early stage of culturing (having better bio-mechanical properties than HA by itself) (83).

Lahiri *et al* have prepared HA/CNT composites by spray-drying; it was proved in this study that wear resistance is improved which results in less debris production. Regarding to cytotoxicity based on osteoblast cells grown on HA–CNT surface it is appointed to be lower than on HA surface (84).

Hahn *et al*, assessed the mechanical and biological performances of HA/CNT composites. HA was heated at 1100°C, and were added to disperse with HA in an acid solution. This dispersion technique introduced -COOH groups on the surface of the CNTs by chemical oxidation (acid solution of H<sub>2</sub>SO<sub>4</sub> and HNO<sub>3</sub>) at 130°C for 30 min. These CNTs were added to a dispersed HA powder and ultrasonically mixed for 2 h. The concentrations of CNTs added to the HA suspension were 1 and 3 wt.% in this study. The evaluation of osteoblasts behaviour was performed by *in vitro* tests; it was found the biocompatibility potential of HA/CNT coatings when compared to HA or Ti coatings, also HA/CNT coatings seemed less cytotoxic to osteoblasts (85).

The above mentioned papers are a great help in defining the most appropriate routes for processing a composite with intact CNTs. However, there is no consensus in the published papers regarding enhancement of mechanical properties as function of the level of CNTs used in the composites. Besides, the electrical conductivity of the composites prepared is not object of study. In terms of biocompatibility, during the last decade synergies between researchers of Europe and United States of America resulted in an extensive publishing of literature on the safety of CTNs. However, these

studies are based on the risk assessment for exposure to CNTs, which can lead to adverse health effects in the target systems: pulmonary, hepatic and cardio-vascular (67, 69, 70, 86). One of this case reports showed bronchiolar and interstitial lung disease on people exposed to World Trade Centre tragedy's dust. Even though, in biomaterials, the toxicity should be assessed on near organs to the implant; an implant dynamic is completely different from breathing dynamic.

When studying the use of CNTs in composites for bone regeneration, the studies of biocompatibility *in vitro* or animal model are limited and not conclusive. These may be a result of differences in the routes used in the preparation of CNTs (79, 81, 83, 85, 87, 88), the way they were functionalized and its purity (59, 71, 89, 90), since most of the papers do not provide extensive characterization of the CNTs and composites used for the biological evaluation reported.

### 3 Materials and Methods

The materials used in this thesis were prepared by Diogo Mata, a PhD student from DECV- Universidade de Aveiro. A P<sub>2</sub>O<sub>5</sub>-CaO glass reinforced based material, composed of hydroxyapatite and tricalcium phases (CaP), was used as a matrix for CaP/CNts composites. These composites were obtained by adding 2.5 wt% of CNTs. The CNTs used were NC7000, supplied by Nanocyl. Purified CNTs were obtained by heat treatment at high temperature and argon atmosphere. The composites were obtained by wet mixing, using a high-speed shear mixing of powders suspensions, and then hot pressure sintered at 1100°C (30MPa), in a inert atmosphere of argon and vacuum. Optimization of all the processing steps to obtain a CaP/CNts composite with good mechanical and electrical properties aiming at bone graft application is the aim of Diogo Mata thesis. He had already achieved a densification of 99% for CaP samples and 93% for the composite. CaP/CNTs samples have also good electrical conductivity properties ( $1.51\Omega\cdot\text{cm}^{-1}\pm0.05$ ) when compared to the CaP samples –  $1.3\times10^{-12}\Omega\cdot\text{cm}^{-1}\pm7.1\times10^{-13}$ .

#### 3.1 Physicochemical Characterization

##### 3.1.1 Scanning Electron Microscopy

SEM was performed using JEOL JSM 35C (Noran Voyager) with 15KV of energy and a resolution until 1.2nm. Samples were observed in two different modes (different electron detectors) depending on the purpose: secondary electrons (SE) - low energy focus on 2 or 3nm depth of the sample which is ideal to observe the topography; backscattered electrons (BE) which will construct the image according to the atomic number of the elements (low atomic number correspond to dark zones, high atomic numbers match to light areas).

Samples of 0.5cmx0.5cm of CaP and CaP/CNTs were used, polished as previous described and washed with alcohol 70% and desionized water.

This analysis was conducted in Laboratório de Microscopia Electrónica de Varrimento e Microanálise por Raios-X at Centro de Materiais da Universidade do Porto (CEMUP).

### **3.1.2 X-Ray Diffraction**

X-Ray Diffraction (XRD) is used to characterize the chemical phase composition materials. Powders to the analysis were obtained by crush and mill of the solid samples until obtaining a granule size less than 75 $\mu$ m. Powder diffraction patterns were measured on a Bruker D8 Discover. The data was recorded using a step size of 0.02° and a 0.4 second dwell time. The CaP and CaP/CNTs were compared with each other and with reference phase files.

These assays were developed at Serviços de Caracterização de Materiais da Universidade do Minho (SEMAT-UM).

### **3.1.3 Roughness**

Surface roughness of the samples was measured using Etamic GMBH profilometer with a diamond tip feeler (HommelWerke). The surface parameter used to measure surface roughness was the arithmetic average roughness (Ra). The selection of the cut-off of 0.25mm was done according to DIN 4768.

Six scans were performed (three in each direction as demonstrated in figure 4) for each sample with a scanning distance of 1.5mm, a scanning speed of 0.15mm/s and vertical amplitude of 80mm. Three samples of CaP and three of CaP/CNTs were analyzed (consecutively polished by sandpaper P1000, P1200, P2500 and P4000). They were previously washed with alcohol 70% for 15minutes then with desionized water, and dried.

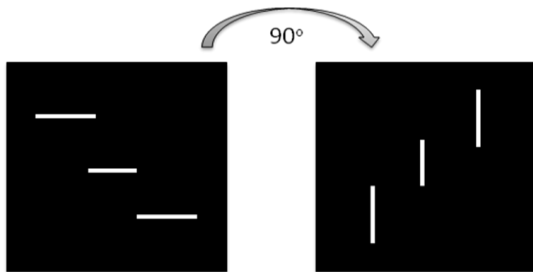


Figure 4 – Scanning scheme of roughness measurements for each sample.

These analysis were performed using the facilities available at Departamento de Engenharia Mecânica of Faculdade de Engenharia da Universidade do Porto.

### 3.1.4 Carbon analysis by Infrared absorption

This test was performed by using LECO TruSpec CHN equipment. Powder with granule size less than 75 $\mu\text{m}$  was used to combustion. About 1g of each material was used to perform a duplicate analysis. The calibration was done with EDTA (certified standard) and the burning temperature was 950°C.

This analysis took place at Laboratório de Caracterização de Resíduos (Centro para a Valorização de Resíduos, Universidade do Minho).

### 3.1.5 Wettability

Contact angles measurements were done on CaP and CaP/CNTs samples polished by a series of water sandpaper P1000, P1200, P2500 and P4000. The samples had 2,5cm in diameter. They were washed with alcohol 70% during 15minutes and then with desionized water (twice). They were dried overnight in a vacuum chamber to avoid humidity interferences with the contact angle measurements.

Wettability was performed using the OCA 15 Optical Contact Angle System (*Data Physics*). It was used the sessile drop method, using a CCD camera (Teli) to record the drop image. The program used was the “SCA20”.

The interaction between material surface and the water, as testing, was monitored for 3 minutes, with a time step of 2s. The sample was placed inside a thermostatted

stainless-steel chamber, with two glass windows of optical quality, and saturated with two pools of the testing liquid – maintaining constant temperature at 25°C (figure 5).

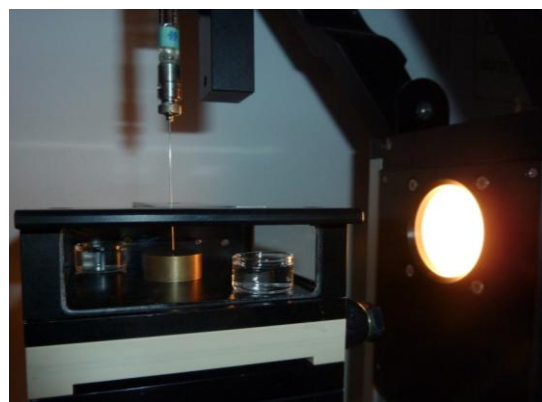


Figure 5 - OCA 15 Optical Contact Angle System (Data Physics, detail of the thermostatted stainless-steel chamber with two pools of water, syringe and illumination.

The drop of desionized water of 4 $\mu$ l was dispensed through a micro-syringe (Hamilton of 500 $\mu$ l) directly on the surface. In each type of material, at least 10 drops were analyzed (two samples of CaP and two of CaP/CNTs) were used. All the drops were placed as shown in the figure 6.

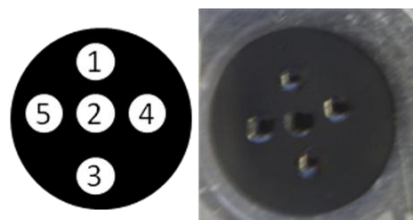


Figure 6 – Scheme with drops order during the experiment.

This assay was carried out at Instituto de Engenharia Biomédica (INEB).

### 3.1.6 Zeta Potential

Zeta potential (ZP) was measured using EKA - Electro Kinetic Analyzer (Anton Paar) equipment with the stamp cell – figure 7. This cell is appropriated to measure zeta potential in solid plan samples with low thickness (less than 3.5mm).



Figure 7 – Stamp cell used with CaP/CNTs samples attached with double-side adhesive tape.

Two samples of each material with the same polish (water sandpaper P1000, P1200, P2500 and P4000), were washed with alcohol 70% for 15minutes then with desionized water (twice) and finally dried in the oven. These samples had dimensions of 20mmx10mmx0.5mm to fit the cell used.

Zeta potential, a measure of the electrical charge of a surface, is estimated from the voltage difference between the solid surface and the bulk liquid phase. The CaP and CaP/CNTs surfaces were exposed to an electrolyte KCl 1mM (Sigma-Aldrich), which contributes to the equilibrium near the surface – figure 8. When the flow starts the mechanical force shears off the layer of counter ions and a charge separation occurs, which is partially compensated by a backflow current (the potential difference is measured).

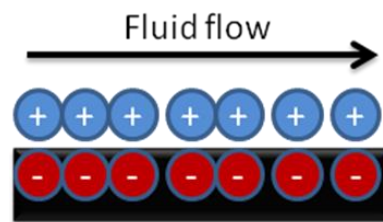


Figure 8 – Equilibrium of ions between solid and liquid phases.

According to the complete zeta potential equation – equation (1), the electrical charge depends on the mechanical force and on the applied differential pressure of the liquid phase ( $dU/dp$ ). Other properties have also high importance such as the viscosity ( $\eta$ ) the dielectric coefficient  $\epsilon \times \epsilon_0$  and the electrical conductivity ( $\kappa$ ) of the liquid phase.

$$\zeta = \frac{dU}{dp} \times \frac{\eta}{\varepsilon \times \varepsilon_0} \times \kappa \quad (1)$$

The EletroKinetic Analyser used had a pH meter (Hamilton Electrochemical Sensor), and a conductive meter (Schott ref. LF613T) to read continuously the pH and the conduction. The temperature was also monitorized. Measurements were performed at least eight times at physiological pH (between 7.1 and 7.3) adjusted with KCl and NaOH (Sigma Aldrich), with a pressure of 400mbar and at an average temperature of 27°C.

These measurements took place at Instituto de Engenharia Biomédica (INEB).

## 3.2 Biological Evaluation

### 3.2.1 *In vitro* conditions

#### 3.2.1.1 Blood compatibility

Haemolysis studies were preformed according to standard ASTM F 756 -00 (2004).

The materials tested, CaP and CaP/CNTs, was crushed and milled until obtaining granules size of 250 to 500µm, then washed with alcohol 70% and with desionized sterile water.

Blood was obtained from healthy volunteers by venipuncture and collected in tubes containing citrate as anticoagulant – fig.9a. The hemogram was obtained with 10µl of complete blood on Micros 60 (ABX HORIBA).

A dilution of 1:100 with water was prepared to obtain a haemoglobin concentration of 800mg/l. By eight consecutive double dilutions with water, it was made a set of seven lysate standards with values from 800 to 12.5mg/l. The absorbance of each solution was read at 540nm, with water as a blank. A calibration graph was prepared by plotting the readings of absorbance (on y axis) against

haemoglobin concentration (on x axis) on arithmetic graph paper, and the slope was drawn (this must pass through the xy origin).

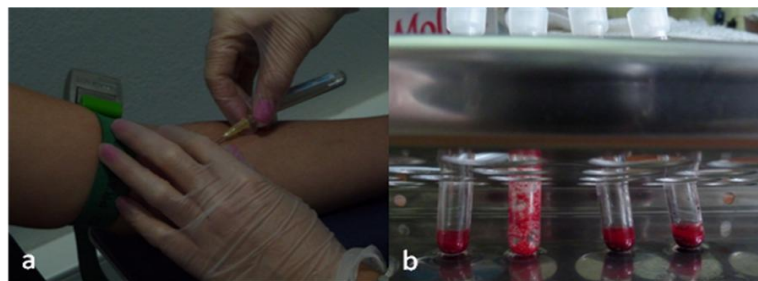


Figure 9 - a) Venipuncture and collection of blood to citrate tubes, b) tubes to each type of blood: negative control, positive control, CaP and CaP/CNTs.

From a normal blood sample, it was prepared a blood solution with 8g/ml of haemoglobin in PBS. From this solution of 8g/ml, 500 $\mu$ l of blood were added to each tube: negative control (empty tube), positive control (tube+100mg of nitrile), CaP (tube+100mg) and CaP/CNTs (tube+100mg) – fig .9b. According with the standard, at least six different bloods must be studied to validate the results therefore 24 tubes were incubated at 37°C with the slower stir.

This experiment was developed at Serviço de Bioquímica of Faculdade de Farmácia da Universidade do Porto.

### 3.2.1.2 Optimization of the electrical stimulation conditions

Aiming the optimization of the electrical stimulation namely current intensity and stimulation time, some experiments were done culturing MG-63 cells on cell culture plates. This method, using salt bridges, is applied by direct supply of current (2 V) to titanium electrodes soaked in saline KCl solutions. These solutions were in contact with the medium via KCl in agar-agar bridges (2.5 g KCl; 7.5 g Agar-agar/100ml of distilled water) allowing the conduction of current through the cell culture – figure 10a. Salt bridges were filled immediately after agar-KCl sterilization. To avoid changing properties, saline bridges were constantly maintained under KCl solution – figure 10b.

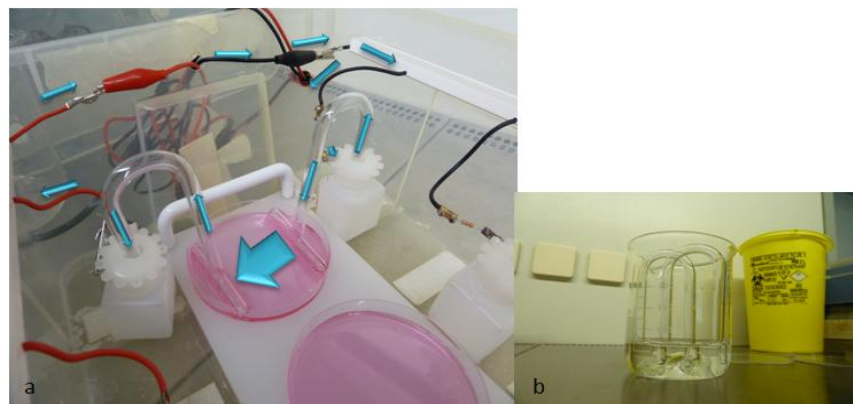


Figure 10 – a) Current flow of cell culture stimulation, b) agar-KCl bridges soaked in KCl solution.

Alternate current (AC) was used (quadratic wave of 40-60 of asymmetry) with frequency of 20Hz. The resistance used differed according to the final current intensity desirable.

#### 3.2.1.2.1 Cell Culture

MG-63 cells, originally isolated from a human osteosarcoma, were used in these experiments. Cells were routinely cultured at 37°C in a humidified atmosphere of 5% CO<sub>2</sub> in air, in 58cm<sup>2</sup> treated-plates (Corning) containing 10 mL of α-minimum essential medium (α-MEM) (Gibco), 10% fetal calf serum (FCS) (Gibco), and 1% antimicrobial (PAA). The medium was changed every third day and, for subculture the cell monolayer was washed twice with phosphate-buffered saline (PBS, Gibco) and incubated with trypsin solution (Gibco) for 5 min at 37°C to detach the cells. The effect of trypsin was then inhibited by adding the complete medium at room temperature. The cells were washed twice by centrifugation and resuspended in complete medium for reseeding and growing in new culture plates.

#### 3.2.1.2.2 Cell Proliferation

The 3-[4,5-dimethylthiazol-2-yl]-2,5-diphenyltetrazolium bromide (MTT) assay was used to measure cell proliferation. MTT is a pale yellow substrate that is reduced by living cells to a dark blue formazan reaction product. This process requires active mitochondria and is thus an accurate measure of the number of viable cells in the culture. To carry out this assay duplicates of 58cm<sup>2</sup> plates were performed to each condition, and seeded with 135x10<sup>3</sup>cells/plate in 10ml of medium and incubated at

37°C and 5%CO<sub>2</sub>. The beginning of electrical stimulation was performed the day after, allowing a correct cell attachment overnight. Medium was always changed every time the plate was stimulated.

Different currents were tested, at first 10µA and 100µA and then, 100µA with 200µA – table 1. In the first experiment it was tested three different stimulation times in order to choose the best option of time and current. Once 15min and 100µA have revealed as the best choice, a higher intensity current was chosen to compare with the previous results. It was also tested the twice a day stimulation of 15minutes. A control of this stimulation was performed; this control (control 15+15) consisted in a plate which came out of the incubator when the other plate was in stimulation. This intended to mimic the impact of low temperature, less CO<sub>2</sub> and all the unfavourable conditions that occur during the application of the stimulus, which may compromise cell growth.

Table 1 - Current and time conditions tested with MG-63 cells.

Experiment	Currents (µA)	Time (min)
1 <sup>st</sup>	10	15
	10	30
	100	60
	100	15
	100	30
	100	60
2 <sup>nd</sup>	100	15
	100	15+15
	no stimulation	Control 15+15
	200	15
		15+15
	no stimulation	Control 15+15

The electrical stimulation took place on a flow laminar cabinet within a device developed by Diogo Mata shown in figure 11. This device consists of a removable platform where three culture plates could be placed, and six containers with a titanium electrode soaked in 0.33M KCl solution. The electrodes are linked to a source of current. Containers have a hole on top to introduce the saline bridge which will

connect the current from the KCl to medium and, consequently, to cells. This connection is possible because these bridges are filled with a solution of Agar/KCl.

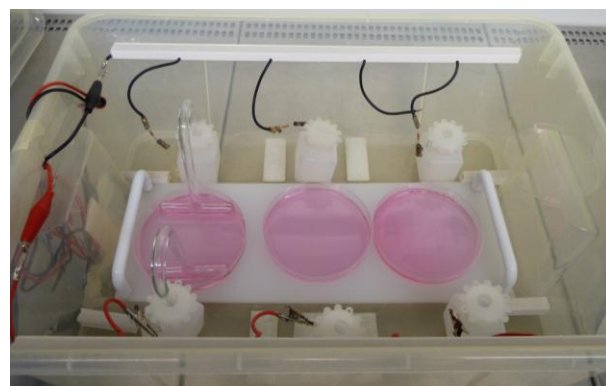


Figure 11 – Electrical Stimulation device.

### 3.2.1.2.3 Statistical Analysis

Duplicate culture experiments were performed, and in each experiment 8 replicates were tested; the median values of the MTT were used to calculate the arithmetic means of the cell proliferation or viability plus or minus the standard deviation (SD). The study of the statistical significance of the results was performed by analyzing variances (ANOVA) -  $p < 0.05$ .

These part of the work was developed at Faculdade de Ciências da Saúde (Universidade Fernando Pessoa).

### 3.2.1.3 Dye Interaction with materials

Once samples are black, some tests were performed in order to quantify a possible influence of the colour on the proliferation assay (MTT), total protein content and alkaline phosphatase (ALP) with and without electrical stimulation.

An experiment with daily 15 minutes stimulation at  $100\mu\text{A}$  was performed on CaP and CaP/CNTs samples. Samples were washed with alcohol 70% (15min), with desinized sterile water (30minutes) and a pre-immersed in PBS for 60minutes. After that, samples were incubated in 24-well plates (Corning) at  $37^\circ\text{C}$ , 5%  $\text{CO}_2$ , with 10 mL of ( $\alpha$ -minimum essential medium ( $\alpha$ -MEM) (Gibco), 10% fetal calf serum (FCS)

(Gibco), and 1% antimicrobial (PAA)), changed every third day. The medium of plates electrically stimulated was changed every day after stimulation to reduce the risk of contamination. Duplicates without stimulation (days 0, 1 and 7) and samples with stimulation (days 1 and 7), were done.

After 1 h (day 0), 1 and 7 days of stimulation, it was evaluated the influence of the colour using the MTT assay (Sigma Aldrich) in which 100 $\mu$ l of MTT (5 mg/mL) was added to each well and incubated at 37°C for 4 h. Afterwards, all the liquid was aspirated from the well and was added 1ml of Dimethyl sulfoxide (DMSO, Sigma Aldrich). 24-well plate was slightly agitated until obtaining a uniform colour solution. The solutions were transferred to 96-well plates (Nunc) and the absorbance measured at 545 nm using a (Stat fax 3200, Awareness Technologies). DMSO was used as blank.

Total protein content and ALP samples were washed with PBS and frozen at -20°C and evaluated at the end of the culture time. The total amount of protein present in the material surface was assayed by the Lowry's method with bovine serum albumin used as a standard. The absorbance was read at 750nm (specord 200, Analytic Jena). ALP activity was determined in cell-layer lysates (obtained by treatment of the cultures with 0.1% triton in water) and assayed by the hydrolysis of p-nitrophenyl phosphate in alkaline buffer solution, pH 10.4, and colorimetric determination of the product (p-nitrophenol) at 405nm. Hydrolysis was carried out for 60 min at 37°C (NaOH (1M) was added to stop the reaction).

These assays were also performed at Faculdade de Ciências da Saúde (Universidade Fernando Pessoa).

### 3.2.1.4 Microbiological assays

Once the whole mechanism of stimulation implies a lot of manipulation and a high risk of contamination (figure 12), microbiological growth was assessed and controlled in order to minimize this event.

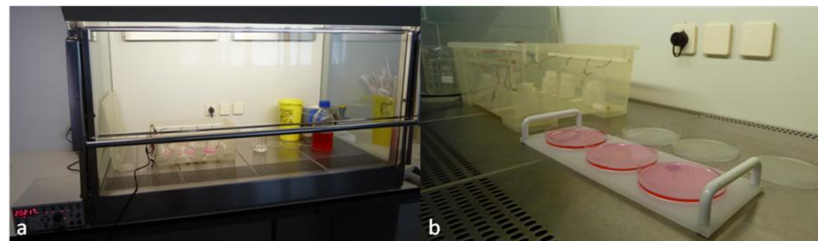


Figure 12 – Stimulation apparatus a) outside the cabinet flow, b) inside the cabinet flow.

In the end of each week of stimulation, one saline bridge had touched a brain heart infusion (BHI) plate and was incubated at 37°C during 24hours. This medium, BHI, is highly nutritious and allow a large spectrum of microorganisms' growth.

When there was bacteria growth, preliminary tests were performed: Gram staining, catalase and oxidase.

#### 3.2.1.4.1 Gram Staining

Gram staining differentiates bacteria according to their membrane system. Gram positive (purple) are the bacteria which have inner membrane, despite gram negative are the bacteria which have an outer membrane above the inner membrane. Bacteria was taken from the colony (with a sterile loop) and put in a lamina with a drop of water. They were dried and fixed at flame (fig.13a,b). Some drops of violet crystal were added (30seconds) – positive colour absorbed by peptoglycans of inner membrane (fig.13c). Then, preparation was covered Lugol solute (60seconds) – fig.13d, and washed with desionized water and with alcohol (96%) to remove violet crystal. In the end safranine was added (30seconds) to dye gram negative bacteria – fig.13e.

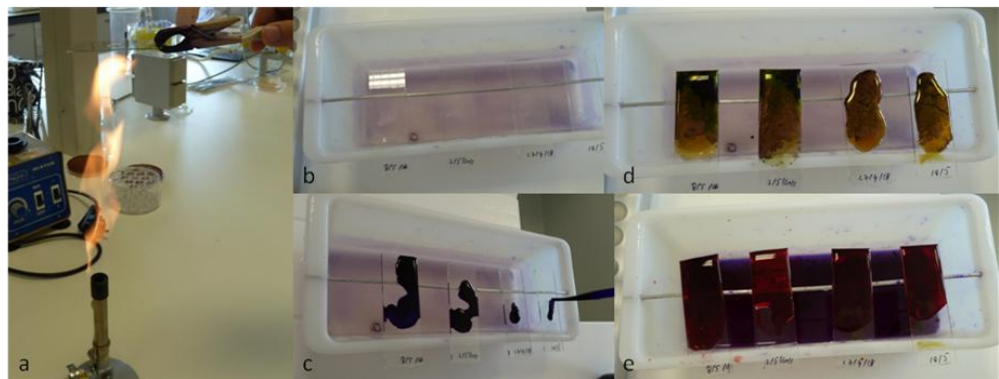


Figure 13 – Gram staining step: a) fixation on fire, b) laminas already fixed, c) addition of violet crystal, d) Lugol solute, e) safranine.

#### 3.2.1.4.2 Catalase test

Catalase assay was performed to detect the presence of catalase enzyme capable of decomposition of hydrogen peroxide into water and oxygen, and it is important to distinguish staphylococcus from streptococcus.

Catalase test was done by placing a drop of hydrogen peroxide on a microscope slide. Using an inoculation loop, it was touched the colony and then smeared a sample into the hydrogen peroxide drop. If bubbles of oxygen were formed, the organism is said to be *catalase-positive* (*Staphylococcus*), if not the organism is *catalase-negative* (*Streptococcus*).

#### 3.2.1.4.3 Oxidase test

Oxidase test is used to find if the bacteria contains cytochrome oxidase or indophenol oxidase. Both catalyse the transport of electrons from donor compounds (NADH) to electron acceptors (usually oxygen). The cytochrome system is usually only present in aerobic organisms which are capable of utilising oxygen as the final hydrogen receptor.

To detect the presence of aerobic organisms the colony was touched with the inoculation loop and touched into the paper disk. It was observed during 3 minutes. If the area of inoculation turned dark blue to maroon to almost black, then the result would be positive (*oxidase-positive*, aerobic organism). If a colour change did not occur within three minutes, the result would be negative.

This microbiological study was also developed at Faculdade de Ciências da Saúde (Universidade Fernando Pessoa).

### 3.2.1.5 Primary Cell culture

To assess the effect of electrical stimulus on cell behaviour, bone marrow cells were grown on CaP and CaP/CNTs samples with and without stimulation. The optimal conditions found in early experiments were applied: 15minutes of stimulation with an alternate current with 100 $\mu$ A of intensity (20Hz of frequency).

Bone marrow cells have fibroblast-like morphology. MSCs were obtained from a young male of 27years old and were bought, cryopreserved from STEMCELL Technologies (France).

Cells were cultured at 37°C under humidified conditions and 5% carbon dioxide (CO<sub>2</sub>). Medium was changed twice a week. When cultures neared confluence, they were trypsinized using 0.05% trypsin. After expansion (13 to 15 days), cells were seeded onto samples at an initial density of approximately 2.8x10<sup>3</sup> cells per sample, with a drop of 50 $\mu$ l. They were incubated for 2hours to allow cells attachment. After that, 1ml of  $\alpha$ -MEM containing 10% FCS, 1% antimicrobial agent (PAA laboratories) 1% ascorbic acid (Sigma), 1% dexamethasone (Sigma), and 1%  $\beta$ -glycerophosphate (Sigma) to induce osteoblastic differentiation.

The bone marrow mesenchymal stem cells grown on CaP and CaP/CNTs samples were analyzed after 1, 3, 7, 10, 14, 21 and 28 days of culture in osteogenic media for cell viability/proliferation and observation by SEM to evaluate cell morphology and matrix mineralization. To each one of these days, cells were fixed and stored to later quantification of differentiation by flow cytometry with BMPR-IB/ALK-6, osteocalcin and collagen type. Flow cytometry protocol is still under optimization to adjust parameters to this type of cells and antibodies.

#### 3.2.1.5.1 Cell proliferation

MTT assay (reduction of 3-[4,5-dimethylthiazol-2-yl]-2,5-diphenyltetrasodium bromide (MTT) to a purple formazan reaction product by living cells) was used to estimate cell viability/proliferation. Cultures were incubated with

100 $\mu$ l of MTT during 4h at 37°C in the incubator; the medium was then decanted, formazan salts were dissolved with 1ml of dimethyl sulphoxide (DMSO) and the absorbance was measured at 545nm in an ELISA reader (96-well plate).

#### **3.2.1.5.2 Statistical Analysis**

Triplicate culture experiments were performed, and in each experiment 8 replicates were tested; the median values of the MTT assay was used to calculate the arithmetic means of the cell viability/proliferation plus or minus the standard deviation (SD). Analysis of the statistical significance of the results was carried out using ANOVA ( $p < 0.05$ ).

#### **3.2.1.5.3 Flow cytometry – cell fixation**

After cell culture, the medium was discarded and the cells were washed with 5ml of PBS. This solution was also discarded after rinsing by agitating the culture plate. 4.6ml of trypsin were added to 58cm<sup>2</sup> culture plate, followed by an incubation step at 37°C for 5 minutes. After that 9.2 ml of medium was added. This cell suspension was transferred to falcon tube centrifuge at 1300rpm for 10minutes. Medium was disposed and 5 ml of washing buffer were added (washing buffer=PBS+2% Fetal calf serum) to resuspend cells. This step was repeated twice. Then the medium was discarded and cells were fixed with 3ml of 1% paraformaldehyde in PBS 1% saponin for 30 minutes. Subsequent to another centrifugation (110rpm, 7min), cells were resuspended in washing buffer and stored at 4°C for future assessment of expression of BMPR-IB/ALK-6, osteocalcin and collagen type I.

#### **3.2.1.5.4 Scanning Electron Microscopy**

For SEM observation, samples were fixed with 1.5% glutaraldehyde in 0.14M sodium cacodylate buffer (pH 7.3), then dehydrated in graded alcohols (from 50% to 100%), and graded hexamethyldisilazane (HDMS) (from 50% to 100%), 10minutes for each solution and overnight evaporation with HDMS 100%. This procedure was performed under hood because of the irritating smell of HDMS. Samples were mounted in a steel base and a gold-palladium sputter-coating was added, with a current deposition of 15mA (to turn the samples electrically conductive) and analysed

in a JEOL JSM 35C (Noran Voyager) scanning electron microscope equipped with a X-ray energy dispersive spectroscopy (EDS) microanalysis capability. It was used 10KV of energy to observe the surface and the thin cells adhered.

### **3.2.2 *In vivo* Conditions**

#### **3.2.2.1 Preliminary subcutaneous screening test**

The aim of this work is to screen subcutaneous tissue reaction of CaP/CNTs composite material compared to the CaP matrix according to ISO 10993-6 and ASTM F1408-97. The screening will be performed after 1 week, 2 and 4 weeks of implantation. However, during this work it was only possible to implant materials in one animal.

One healthy and skeletally mature Merino breed sheep, with an average weight of 50 kg, was used as experimental model. Adequate measures were taken to minimize pain and discomfort and all procedures were approved by the veterinary authorities of Portugal, in accordance with the European Communities Council Directive 86/609/EEC, and by the ICBAS-UP Ethic Commission. This work was performed with the support of “Centro de Estudos de Ciência Animal (CECA), Instituto de Ciências e Tecnologias Agrárias e Agro-Alimentares (ICETA), Universidade do Porto, Campus Agrário de Vairão” and “Instituto de Ciências Biomédicas Abel Salazar da Universidade do Porto (ICBAS-UP)”.

All surgical procedures were conducted under general anaesthesia. A penicillin–streptomycin association was administered pre-operatively to provide antibiotic cover.

The animal was washed, shaved and disinfected on dorsal area – figure 14a. Triplicates of CaP and CaP/CNTs granules (250-500µm) were put in polypropylene open tubes, and implanted subcutaneously in the dorsal midline – figure 14b. Blood from the animal was used to fix the granules inside the tubes. Merino breed sheep was sutured and housed in a recovery cage – figure 14c. The animal will be sacrificed 1 week after surgery in order to evaluate the early responses by histology studies.

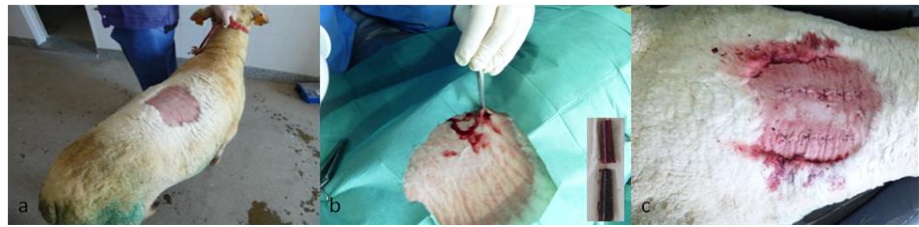


Figure 14 – a) Animal washed, shaved and disinfected in dorsal area, b) Performing the subcutaneous space to implant the open tubes with granules, c) Animal sutured in the end of the intervention.

## 4 Results and General Discussion

### 4.1 Physicochemical Characterization

#### 4.1.1 Scanning Electron Microscopy

Scanning Electron Microscopy (SEM) is important to characterize the topography of the materials since it determines the cell response.

Figure 15a shows a typical microstructure of a CaP sample, which implies that the carbon contamination did not affect the general structure of this material. CaP/CNTs composite showed a homogeneous distribution of CNTs on CaP matrix (fig. 15b), but many clumps of CNTs distributed in the microstructure were observed.

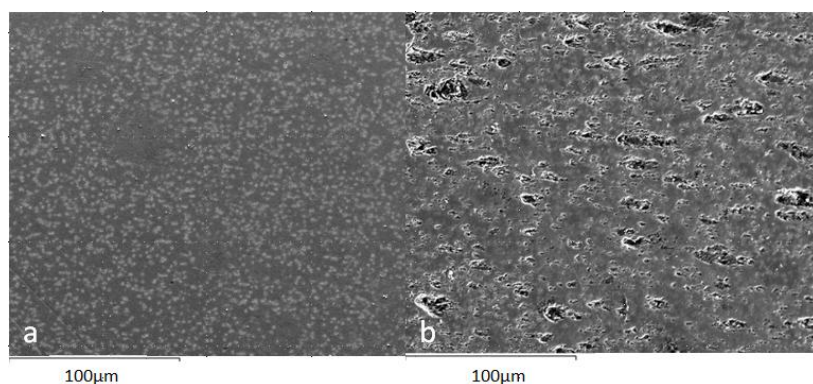


Figure 15 - SEM micrographs of a) CaP and b) CaP/CNTs samples (1000x).

More details about microstructure of CaP and CaP/CNTs composite could be observed in figure 16.

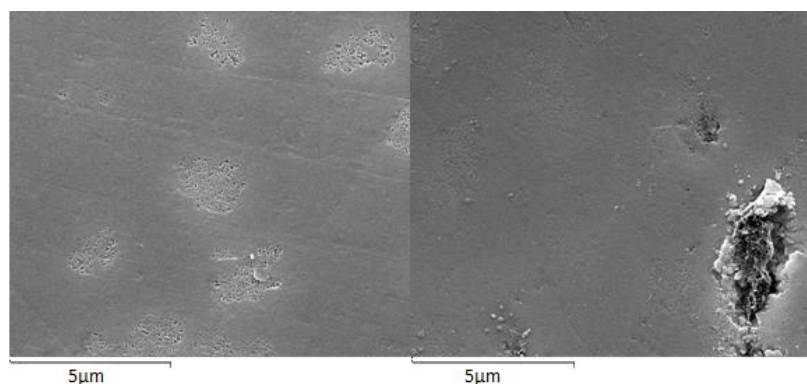


Figure 16 - SEM micrographs of a) CaP and b) CaP/CNTs samples (20000x).

#### 4.1.2 X-Ray Diffraction

X-Ray Diffraction (XRD) was used to identify crystalline phases of CaP and CaP/CNTs samples. Sample patterns are shown in figures 17 and 18. The measured patterns were analysed and compared to Joint Committee on Powder Diffraction Standards. According to these files, peaks were assigned as been HA and  $\beta$ -TCP phases – figure 17. CaP and CaP/CNts spectra were very similar (main peaks of HA JCPDS 72-1243: 31.7°, 32.1° and 32.8°, main peaks of  $\beta$ -tricalcium phosphate, JCPDS 09-0169: 31.0°, 34.4°, 27.8°).

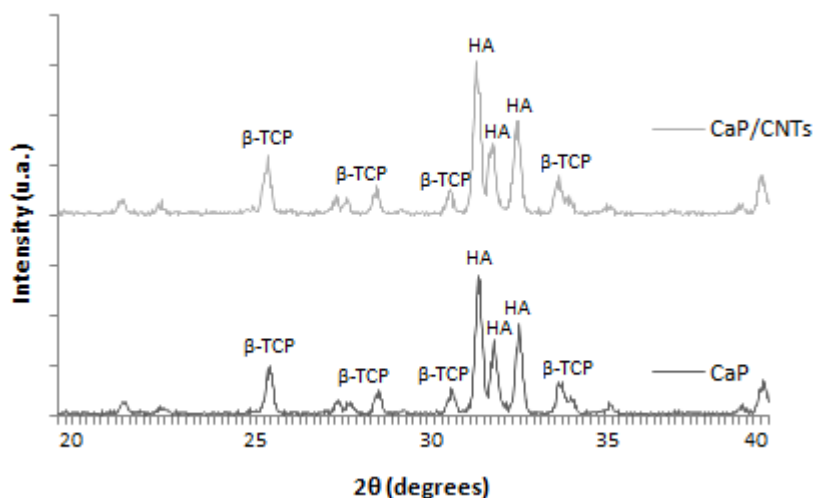


Figure 17 - XRD patterns of CaP and CaP/CNTs materials.

The main peak for graphite in CNTs, which occurs at  $2\theta = 26.6^\circ$  was not observed as shown in figure 18 (91, 92). Since a load of CNTs higher than 1wt% was used, a longer acquisition XRD data may be need to detect the signal. According to JCPDS 9-348 and other studies already reported (93, 94), some other peaks of  $\alpha$ -TCP could exist in this calcium phosphate matrix. These peaks in data range from 29° to 31° were not observed in CaP and CaP/CNTs spectra – figure 18.

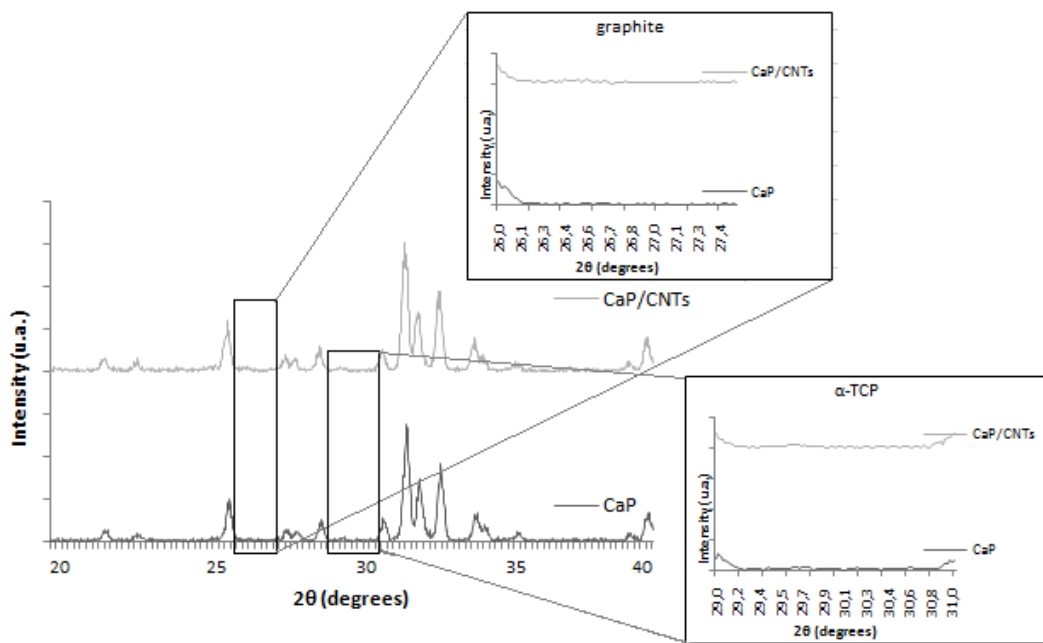


Figure 18 – XRD patterns of CaP and CaP/CNTs materials.

### 4.1.3 Roughness

Several studies seem to agree that some degree of roughness promotes proliferation compared to a smooth surface (95, 96).

An isotropically rough surface was observed since the roughness was independent of direction. CaP samples presented the smoothest surface with an average roughness ( $R_a$ ) of  $0.05 \pm 0.01 \mu\text{m}$

The higher roughness of CaP/CNTs samples (table 2) should be the result of the polishing step of a material which is composed of phases with too different hardness (CaP and CNTs). Clumps of CNTs disposed in CaP matrix should contribute to this higher roughness as other researchers had found the same results (97).

Table 2 - Surface roughness ( $R_a$ ) values for CaP and CaP reinforced with CNTs.

Materials	$R_a (\mu\text{m})$
CaP	$0.05 \pm 0.01$
CaP/CNTs	$0.17 \pm 0.03$

#### 4.1.4 Carbon analysis by Infrared absorption

Carbon content was studied by the combustion-InfraRed absorption method, in order to ascertain the extent of carbon in the samples. On CaP/CNTs samples, this analysis quantifies the carbon provided by the amount of CNTs present and the carbon contamination.

Observing CaP tablets, they present a black colour on the surface – fig.19. Once the mould to compression is made of graphite, some carbon diffusion into the material occurred. From carbon analysis by infrared absorption, values of  $0.96\% \pm 0.04$  and  $2.57\% \pm 0.01$  were obtained for CaP and CaP/CNTs materials respectively – table 3.



Figure 19 – CaP tablets after sintering process.

There are several publications reporting the same problem of carbon contamination due to graphite moulds, although with less percentage of contamination in alumina chromium oxide and alumina zirconia, 0.04 to 0.5w% and 0.06w%, respectively. These reports refer the almost same hot press temperature ( $1500^{\circ}\text{C}$  or  $1450^{\circ}\text{C}$ ) but much less pressure (49KPa contrasted with 30MPA) and less exposure area ( $5$  ou  $9\text{cm}^2$  compared to  $\sim 35\text{cm}^2$  ) than the used in this work (98, 99). Nevertheless, one of the above references admits that sintered samples were grinded down 1 mm each side and an external ring of 0.5 mm was removed before carbon analysis quantification (99).

Table 3 – Percentage (%) of carbon found by infrared absorption on CaP and CaP/CNTs samples

Materials	% of Carbon
CaP	0.96
CaP/CNTs 2.5w%	2.57

#### 4.1.5 Wettability

Wettability is a very important property of the solid surface in practical applications. It is governed by chemical composition and by the geometrical microstructure of the contact surface.

Water contact angle was measured for CaP and CaP/CNTs samples and the results are presented in table 4.

On CaP samples hydrophilic behavior was observed, with a contact angle average of  $61.5^\circ \pm 1.6$ . Similar behavior was already observed for instance by *M.A. Lopes* and co-workers (94) and *Wongwitwichot* and collaborators (100).

Once the graphitic carbon was reported as superhydrophobic -  $156^\circ$  (101) and pristine CNTs are inherently hydrophobic (reporting data range  $144^\circ$  to  $156^\circ$ ) (102), it was expected an higher contact angle for CaP/CNTs compared to calcium phosphate. It was observed a slight hydrophobicity with a contact angle average of  $96.6^\circ \pm 3.7^\circ$ , which confirms the hydrophobic power of CNTs even when used loads in a composite (2.5w%).

Table 4 - Contact Angles of water on CaP and CaP/CNTs samples ( $\theta$ ).

Materials	Contact Angles ( $\theta$ )
CaP	$61.5^\circ \pm 1.6$
CaP/CNTs	$96.6^\circ \pm 3.7^\circ$

#### 4.1.6 Zeta Potential

Zeta potential (ZP) is an indirect measurement of surface charge. It is a relevant parameter since it determines the interaction of the surface with proteins, and therefore affects the adhesion and growth pattern of cells.

The zeta potential of CaP and CaP/CNTs materials is shown in table 5. The calcium phosphate showed a value of  $-25.4^\circ \pm 2.0^\circ$ , which is consistent with the bibliography (94).

Table 5 - Zeta potential values for CaP and CaP reinforced with CNTs (mV).

Materials	Zeta Potential (mV)	pH
CaP	-25.4±2.0	7.17±0.04
CaP/CNTs	-1.3±0.3	7.17±0.05

Zeta potential of carbon nanotubes is function of its purity and functionalization. The values published for pristine MWCNTs are dispersed (from 0mV to -29.3mV, pH=7), probably due to different purities, but major of the times higher than the reported value of CaP materials, which supports the measurement (103, 104). The zeta potential value found to CaP/CNTs confirms the absence of organic groups (CNTs non-functionalized), which would have to reduce zeta potential value when compared to CaP.

## 4.2 Biological Evaluation

### 4.2.1 *In vitro* conditions

#### 4.2.1.1 Hemolytic Properties

Haemolysis is the rupturing of erythrocytes, and the release of their contents (for example haemoglobin) in blood plasma. This reaction could be induced by extracorporeal materials which activate some receptors triggering their death. Consequently, even not mandatory by ISO10993-Part1, this study should be done once the material will be implanted in animals or humans.

According to standard ASTM F756, there is an haemolytic grade (table 6) which makes a distinction between types of materials. If the haemolytic index is between 0% and 2%, the material will be nonhemolytic, and the data range from 2% to 5% indicates a slight haemolysis. If the haemolytic index is superior to 5%, the material is considered haemolytic and could not be implanted. This assay is only

obligatory and crucial to cardiovascular devices, although it is always a good clue to the *in vivo* material behaviour.

Table 6 – Hemolytic grade according to standard ASTM F756.

Hemolytic index above the negative control	Hemolytic grade
0-2	nonhemolytic
2-5	slightly hemolytic
>5	Haemolytic

For CaP samples a percentage of haemolysis of 4% was obtained (fig.20). This slightly haemolytic behaviour has already been reported (105).

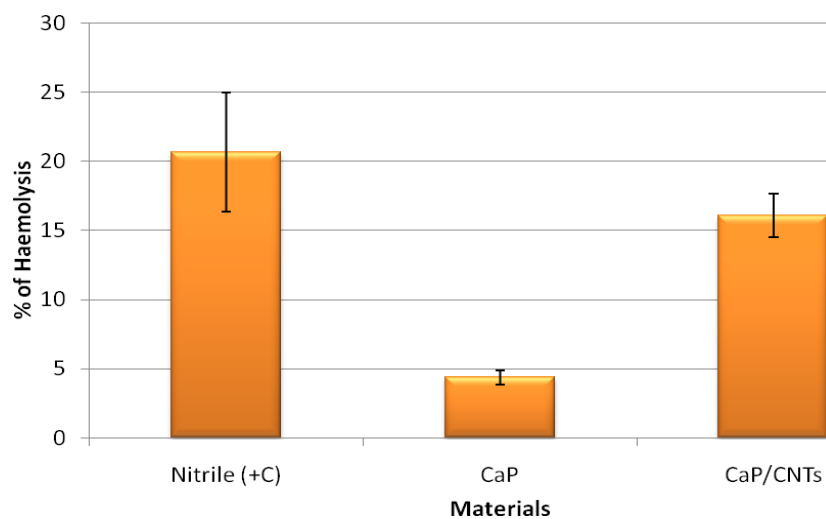


Figure 20 – Percentage of haemolysis of each material: nitrile (positive control), CaP and CaP/CNTs.

The haemolysis found on blood (negative control) was subtracted to all the conditions (normal haemolysis).

However, CaP/CNTs samples showed a much higher haemolysis than the baseline presented by the standard; therefore this material seems to be very haemolytic (16%) – fig.20.

In figure 21 are represented micrographs of one of the bloods analyzed. In fig. 21a, it is shown the red blood cells (RBCs) normally round (negative control), although in fig. 21b a lot of deformed RBC can be seen due to the action of nitrile (positive control – induces lysis). In figure 21c, which correspond to blood that have interacted with CaP granules, some RBCs are not as round as normal, previewing the lysis of 4%. In figure 21d some cellular debris can be visualized indicating an extensive that lysis (16%).

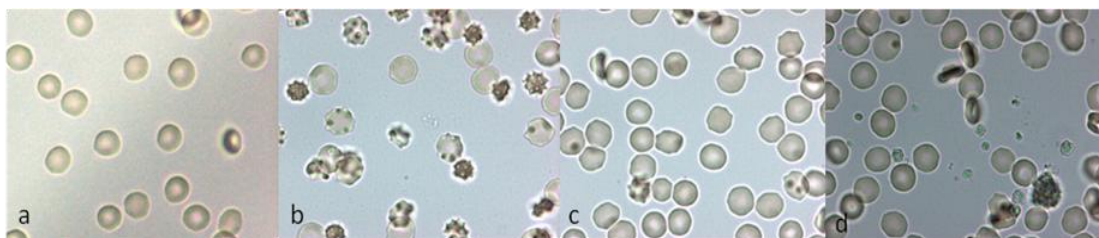


Figure 21 – Optical microscopy pictures of a) blood – negative control, b) blood with nitrile - positive control, c) blood in contact with CaP, d) blood in contact with CaP/CNTs. All the samples have a dilution of 1:10 and an augmentation of 1000x (oculars + objectives).

Some published studies showed other perspectives. Authors have reported MWCNTS to cause an haemolysis less than 5%, but using different testing conditions; the interaction time between blood and material was just 60 seconds and the blood used was from rabbit (without agreement with standard) (106). Platelet adhesion studies on nanocrystalline diamond coatings found diamond like carbon to be non trombogenic (107). So, the haemolysis index of the CaP/CNTs composite may depend on the testing conditions.

The incubation conditions for hemolysis testing as suggested by standard F756, may not be adequate to the type of biomaterials under assessment (highly diluted blood; 100% static incubations is not possible due to sedimentation of red blood cells – RBC) (108). In fact, in this work one of the bloods was tested under two different conditions: with dynamic movement, in static incubation). There were no differences for CaP material incubation, though for CaP/CNTs composite the haemolysis under dynamic incubation was 3% higher than the static experiment. This may demonstrate the contribution of movement to the liberation of some compounds or particles which may contribute to haemolysis. Despite the high purity of the CNTs used in the CaP/CNTs composite, the release of some ions from CNTs such as iron to

the medium may have caused hemolysis ; it is known that iron induced intravascular haemolysis (109). The release of CNTs from the composite is also a possibility during the exposition of the composite to blood with stirring. Since Nanocyl CNTs used in this work have small size and high aspect ratio ( $>150$ ; average length of  $1.5\mu\text{m}$  and an average diameter of  $9.5\text{nm}$ ) once released they could just act as needles and burst red blood cells, which have a diameter of  $8\mu\text{m}$ . The higher hardness of CaP/CNTs composite compared to CaP material may also have led polygonal granules to damage erythrocytes (fig. 22).

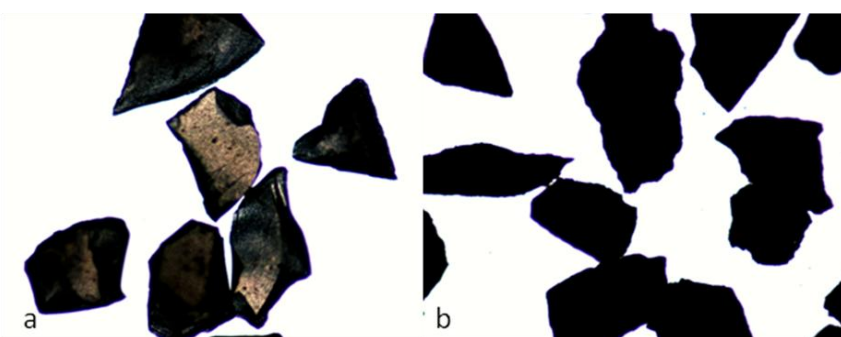


Figure 22 – Optical microscopy images; a) CaP granules of  $250\ \mu\text{m}$  to  $500\mu\text{m}$ , b) CaP/CNTs granules of  $250\mu\text{m}$  to  $500\mu\text{m}$ . (Augmentation of 100x (objectives +oculars)).

Further *in vivo* studies using an animal model should better clarify the blood compatibility of CaP/CNTs composite.

#### 4.2.1.2 Optimization of the electrical stimulation conditions

In order to determine the best conditions of electrical stimulation as intensity of current and stimulation time, electrical stimulus were applied to MG63 cultured on plastic culture dishes.

Figure 23 shows the results of the first experience performed. It was found that 30minutes of  $100\mu\text{A}$  stimulation is similar to a normal growth without any stimulation (control). The majority of the tested conditions are statistically different from the control, although only one condition have revealed higher proliferation of cells – 15minutes,  $100\mu\text{A}$ . In general, better results were obtained to cells stimulated at  $100\mu\text{A}$ . It was also found that as time of stimulation increases, the number of cells

decreases. This could be explained because of the higher exposure time to unfavourable conditions (temperature about 25°C and low percentage of CO<sub>2</sub> in the air of the laminar flow cabinet). With this experience it was found out that there was a threshold of benefit exists. At 100µA, on 5<sup>th</sup> day, 15minutes obtained better results than the control; 30minutes was very similar to the control, and 60minutes of stimulation was worse than the control. In ideal conditions, 30minutes of stimulation should be better than 15minutes, though it had not happened because of the hostile environment.

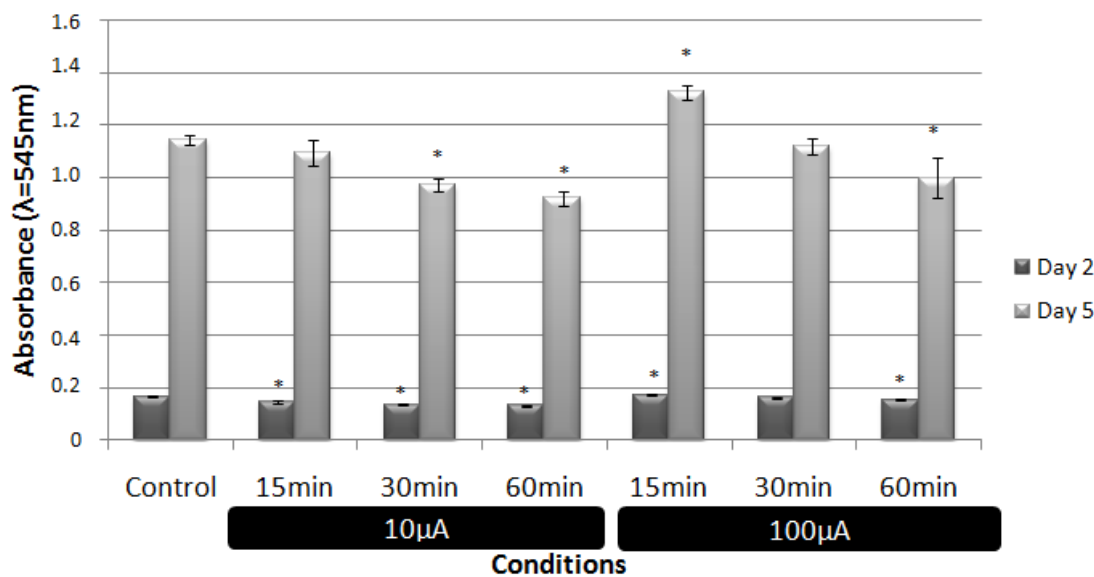


Figure 23 – Effects of 10µA and 100µA electrical stimulus and application time (15,30 and 60min) on the growth of MG63 cells. MG63 cells were grown on two replicates of plastic culture dishes of 58cm<sup>2</sup>. MTT assay was carried out and the absorbance was read at 545nm. The bars show the averaged of two separate experiments ± SD (vertical lines). \*: Statistically different from the control ( $P \leq 0.05$ ).

Since 100µA and 15minutes of electrical stimulation showed better results to cell growth, another experiment was performed to compare this intensity with an higher intensity of current, and to compare a single stimulation of 15minutes with a twice a day stimulation of 15minutes. Furthermore, a control without stimulation was prepared to came out from the incubator during the stimulation of 15+15minutes to be exposed to the adverse circumstances in order to quantify how these conditions are deleterious to cells.

The outcome of the second experience is presented in figure 24, where the majority of the results are statistically different from the control. By comparing times

of stimulation, it was found that the optimum period was 15minutes of cell stimulation once a day. 15+15minutes of stimulation have demonstrated a lower number of cells than control. As the 15+15minutes control presented similar behaviour on cells stimulated with both different currents of stimulation, it was demonstrated that the bad influence of unfavourable conditions (low temperature and percentage of CO<sub>2</sub>) overrides the beneficial effect of electrical stimulation. Comparing the results of the two experiments is also visible a worse growth at 15+15minutes than at 30minutes. This event could be explained by the effective time out of the incubator. A 15+15minute experiment leads cell culture plates be one hour outside of the incubator (30min stimulation + 30min of preparation and changing media), though the 30 minute stimulation corresponds roughly to 45 minutes out of the incubator.

Regarding to the current's intensity, even 15min of stimulation (200µA) was superior to the control; 15 minutes with 100µA had the best performance reaffirming the conditions found out in the previous experiment.

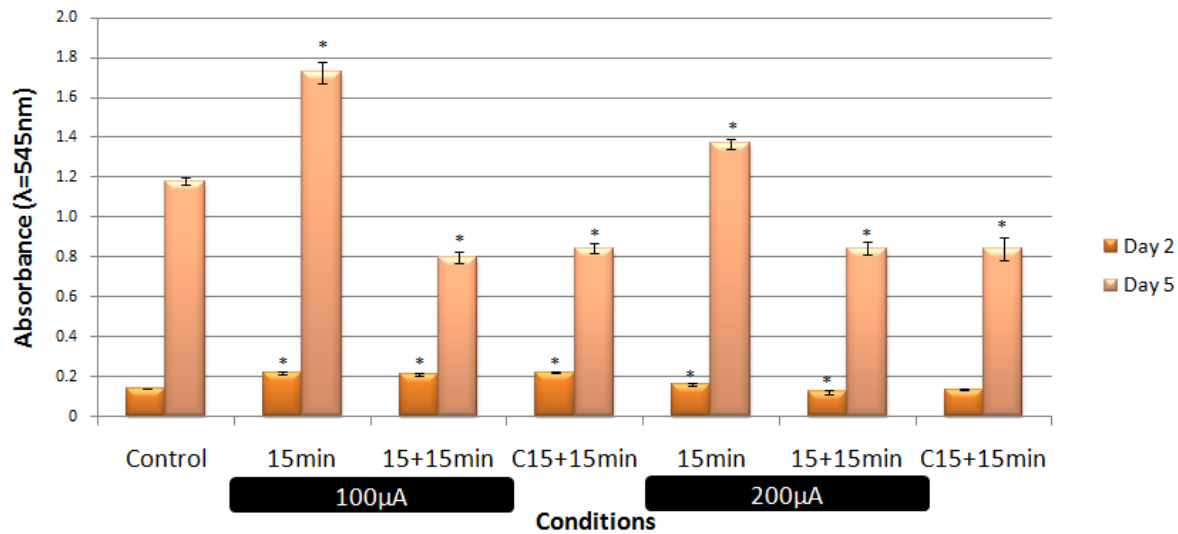


Figure 24 - Effects of 100µA and 200µA of electrical stimulus and application time (15 and 15+15min) on the growth of MG63 cells. MG63 cells were grown on two replicates of plastic culture dishes of 58cm<sup>2</sup>. MTT assay was carried out and the absorbance was read at 545nm. The bars show the averaged of two separate experiments ± SD (vertical lines). \*: Statistically different from the control ( $P\leq 0.05$ ).

#### 4.2.1.1 Dye-Interaction with materials

Once materials were black, possible interactions between materials and chemicals from cell culture tests were evaluated. Acellular assays were performed with and without electrical stimulation. The results for MTT tests are shown in figure 25a for CaP samples and in figure 25b for CaP/CNTs composite.

CaP black samples presented higher interaction with MTT on day 0, possibly due to the release of carbon (from the contamination). On day 1 and day 7, all samples presented a small signal, which may not interfere in cell culture results (~0.02). To overcome this situation the pre-immersion on PBS must be performed for 24hours.

Non stimulated CaP/CNTs samples showed a constant interference although stimulated CaP/CNTs samples showed a decrease with time. Even though, the interference signal is negligible when compared with normal MTT cell results.

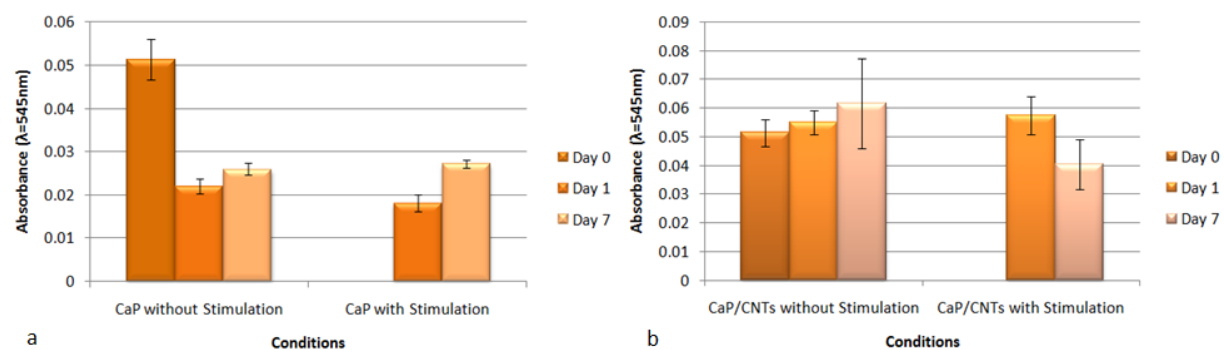


Figure 25 – MTT interaction with a) CaP samples, b) CaP/CNTs samples.

Total protein content assessed on acellular medium that contacted CaP and CaP/CNTs samples revealed an absence of signal as expected, and therefore no interference occurred. All the samples, stimulated and non-stimulated on day 1 or day 7, presented zero content of total protein. Summarizing this test could be applied in this work, without any chance of interfering processes. However, regarding the ALP quantification, in similar conditions, very different results were obtained – figure 26. Independently of the material, time or day of assessment, all the results were excessively high and invariable. Once there were no proteins in the samples, some interference between material and assessment solutions should not have happened. Therefore, this assay was excluded from the assessment of differentiation methods.

Total protein content test was also eliminated because it is used to normalized ALP test.

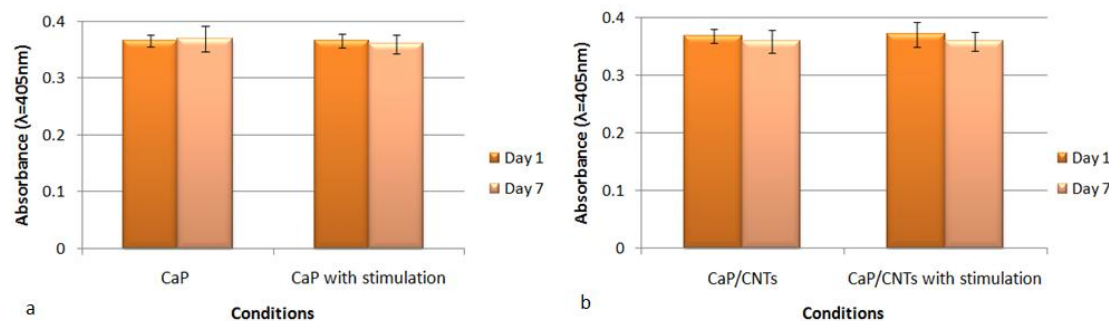


Figure 26 – ALP interaction with a) CaP samples, b) CaP/CNTs samples.

With these preliminary studies, colorimetric tests to evaluate osteoblasts differentiation were abandoned and replaced by flow cytometry, which is a more sensitive and reliable method.

#### 4.2.1.2 Microbiological assays

In order to assess the microbiological growth in the saline bridges and supervise adequate practices in the experiments with stimulation, microbiological assays were performed, and the results are presented in table 7. Saline bridges were incubated in brain heart infusion plates (BHI), and some basic characterization was developed in order to identify the type of contamination.

Table 7 – Microbiological growth in BHI plates.

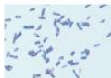
Material	Conditions	Time	Growth	Picture
Saline bridges	KCl sterile (changed every 3days)	7 days	no	
Saline bridges	KCl sterile (changed every 3days)	15days	yes	
Saline bridges	KCl sterile with antimicotic and antifungic solution	20 days	yes	
Saline bridges	KCl sterile (changed every 3days)	20 days	yes	
KCl from the electrodes bottle	KCl sterile (changed every week)	20days	no	
Saline bridges	KCl sterile (changed everyday)	15 days	yes	

After 7 days of bridges filling, and soaking in KCl changed every third day, there was no microbial growth. Although after 15days a lot of microorganisms have grown. By gram staining it was found bacteria rods gram-positive and negative which are also *oxidase-positive* (table 8). Facing this situation, the idea was to add the same antimicrobial solution (PAA laboratories), used in the cell culture medium to the KCl solution. On the day 19<sup>th</sup>, 10ml/L of antimicrobial solution was added to the soaking solution. 24hours later this saline bridge and another without antibiotic addition were incubated in BHI plates. The results were satisfactory growing only two colonies on the plate from the saline bridge with antimicrobial solution. The single colonies were gram-positive rod. Although on the plate incubated without antimicrobial solution, were found gram-positive *cocci* and *catalase-negative* bacteria, which should be from a *Streptococcus* lineage. These results prove a large spectrum of bacterial growth on saline bridges. The author concluded that this approach could be successful if performed during the filling of the bridges. Besides that, it was also checked if there was microbiological growth in the KCl of the electrodes bottles. Few drops of this solution (one week old) were incubated at 37°C during 24h (BHI plates), revealing no growth. This was acceptable once this solution is less exposed to manipulation and contamination.

After these observations, saline bridges were sterilized and refilled, and soaked every day in new sterile KCl solution with 10ml/L of antimicrobial solution. After 15 days of this procedure the microbial growth was again assessed as previously described. Still bacterial growth was observed after 24h of incubation (negative rods and *positive-oxidase*) – table 8.

The ideal solution would be the addition of the antimicrobial solution to agar-KCl solution during its preparation. However, as this solution is sterilised at 120°C it is not possible to do it. Therefore it was decided to increase the concentration of the antimicrobial solution aiming to retard as much as possible any contamination.

Table 8 - Microbiological assays of organism's growth.

Material	Time	Gram staining	Picture	Oxidase	Catalase
Saline bridges	15days	Positive and negative rods		Negative	Positive
Saline bridges	20 days	Positive cocci		Positive/Negative	Negative
Saline bridges	20 days	Positive rods		Negative	Negative
Saline bridges	15 days	Negative rods		Positive	Positive

#### 4.2.1.3 Primary cell culture

Human primary cells are preferred over transformed or immortalized cell line because they are more representative of cells *in vivo*. A typical human bone marrow cells experiment was performed for 28 days with the optimized conditions of intensity of current and stimulation time previously defined.

Carbon-based biomaterials are not new and known by their chemical inertness and biocompatibility and have been proposed for several applications in biomedical field (111-113). Besides carbon is an element in the human body and therefore CNTs entrapped in a calcium phosphate structure are not expected to have any deleterious effect on cells growth and differentiation.

The results of cell viability/proliferation (MTT assay) are presented in figure 27. Cells grown on non electrical stimulated samples (CaP and CaP/CNTs) showed similar patterns, but less cell growth than in the control (absence of materials, standard polystyrene tissue culture plates) which corresponds to a tissue culture treated plastic for cell culture. Until day 7, CaP/CNTs material under stimulation led to the highest cell culture growth values (statistically different and superior from the control) suggesting a beneficial effect of electrical stimulation in cell growth. From the 10<sup>th</sup> day to 14<sup>th</sup> day, cells grown on CaP/CNTs samples are not statistically different from the control, but they are statistically different and higher than the other materials. On day 21 of cell culture, it was attained the maximum proliferation of cells for all material under test. On the last day of the experience (28d), a decreased in cells proliferation for all material was observed, which is supported by the osteoblasts differentiation. Osteoblasts start their differentiation by producing a collagen membrane with osteocalcin and osteopontin. After that, osteoblasts are ready to mineralize by the deposition of hydroxyapatite crystals. The osteoblasts trapped in the calcium phosphate matrix (osteocytes) are characterized by a low metabolic activity therefore they do not metabolize the MTT molecule, which decreases the MTT signal.

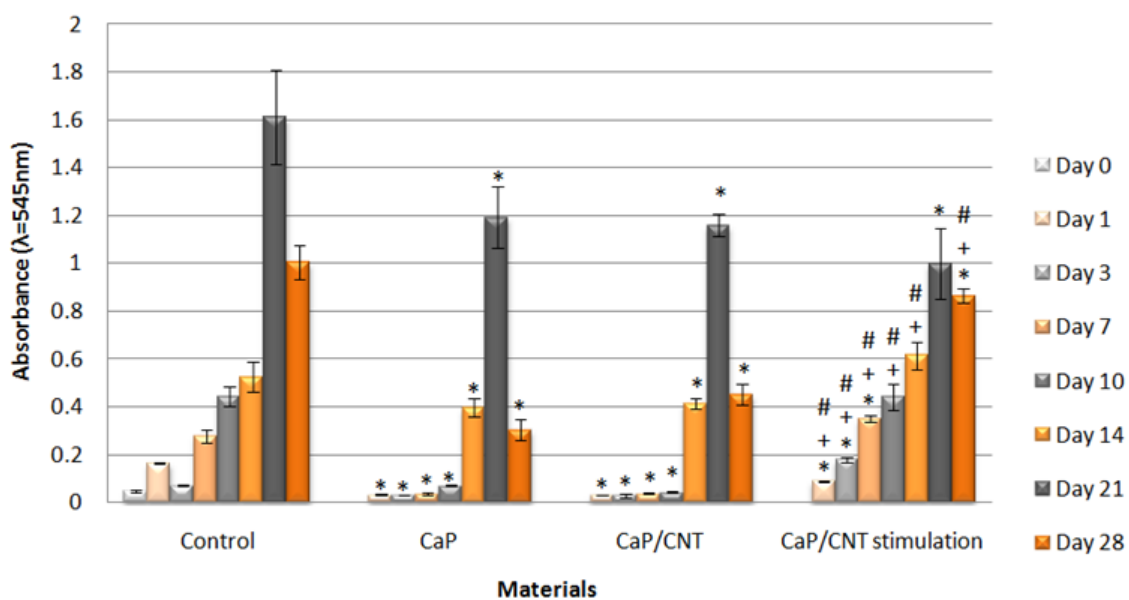


Figure 27 – Cell proliferation of human bone marrow cells grown on polystyrene treated plates, CaP and CaP/CNT samples with and without stimulation for 28 days. \*: Statistically different from the control, + statistically different from the CaP, #: statistically different from the CaP/CNT ( $P \leq 0.05$ ).

As shown in figure 27, CaP and CaP/CNT samples, in the presence or not of stimulation, had similar cell proliferation patterns despite their differences in

arithmetical mean roughness ( $0.05\mu\text{m}\pm0.01$  and  $0.17\mu\text{m}\pm0.01$ , respectively), which indicates that roughness values are in a range that do not seem to affect to cell adhesion and growth.

As above mentioned CaP/CNTs composite has a more hydrophobic surface and less negative than CaP material surface. Proteins of physiological fluids are known by present a hydrophobic folding and negative charge at physiological pH, which favoured proteins adsorption to CaP/CNTs surface compared to CaP material surface (114). However, as can be concluded from the MTT assay results, this adhesion was not strong enough to hamper cell adhesion and proliferation.

Microscopy Electron Scanning was carried out in order to visualize the morphology of cells and to perform a follow-up of their growth. Samples were dehydrated with hexamethyldisilazane (HDMS) due to an unavailability of critical point drier equipment.

SEM observations showed that cells were well spread after 3 days of experiment – figure 28a. At the 10<sup>th</sup> day of culture, cells seeded on CaP samples were well spread and had completely covered the surface (fig. 28b). Even though, some problems may have happened with the preparation technique to SEM, and the follow-up for all the times and materials was compromised. Nevertheless, several authors suggest HDMS drying instead of critical point dry, obtaining the same or better results with this chemical dehydration (115, 116). As seen in figure 28c, in some samples only a few cells were observed, and they seem partially destroyed. Since warnings suggested about the usage of HDMS namely the temperature, the number of hours of exposure (117) has been followed, the reason may be in using a glutaraldehyde solution not recommended for use as an electron microscopy fixative.

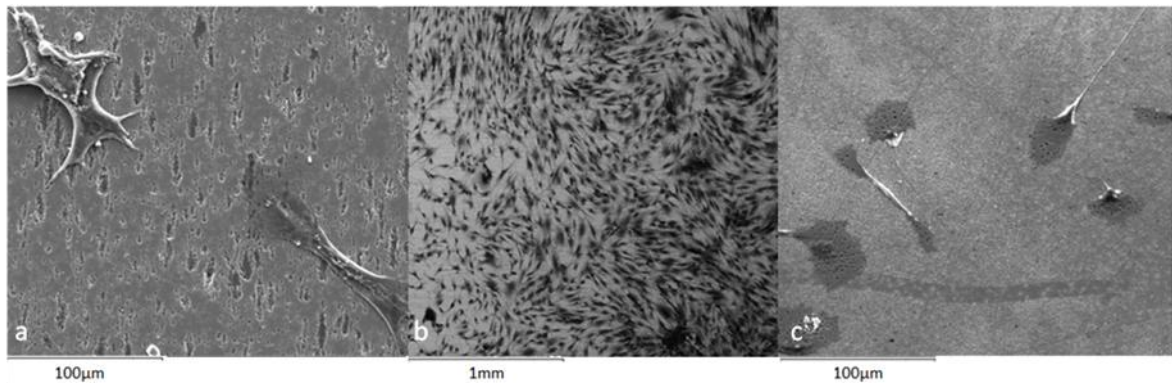


Figure 28 – Scanning electron microscopy micrographs a) spread cells on CaP/CNTs samples on 3<sup>rd</sup> day, b) 10<sup>th</sup> culture day on CaP surface, c) Damaged cells on CaP samples after 7days of culturing.

#### 4.2.2 *In vivo* conditions

The *in vivo* subcutaneous studies are still ongoing and no histological results are yet available.

## 5 Concluding remarks and future work

### 5.1 Conclusions

This work focused on the physicochemical characterization of a novel calcium phosphate matrix reinforced with carbon nanotubes (CaP/CNTs) as well as on the assessment of its biocompatibility through *in vitro* cell culture and preliminary *in vivo* assays. The inclusion of CNTs with high purity into a calcium phosphate matrix by a controlled sintering process reduced the wettability and increased the zeta potential of the composite compared to the CaP matrix, but brought electrical conductivity to the CaP/CNTs composite. The latter effect is crucial for bone regeneration and surpasses the others, as demonstrated by the osteoblastic cells response to the AC current stimulus compared to CaP matrix and CaP/CNTs composite not electrical stimulated.

The *in vivo* subcutaneous studies are still ongoing and no histological results are yet available.

From the interesting results obtained up to now the novel composite material seems to have potential to be used in bone graft field, still further studies are needed.

### 5.2 Future Work

In the very near future protocols for flow cytometry to assess BMPR-IB/ALK-6, osteocalcin and collagen type I expression should be ready to use. Then, cells grown on CaP/CNTs and CaP materials during the experimental work of this thesis that were storage will be evaluated to assess the effect of electrical stimulus on the level of expression of the above mentioned proteins, and therefore quantify the effect of electrical stimulus on cell differentiation.

*In vivo* subcutaneous reactions will be assessed by histological preparations, in order to evaluate the immunological response and biocompatibility of CaP and CaP/CNTs materials.

Regarding the haemocompatibility evaluation, other studies besides the haemolytic tests already done such as coagulation studies will be performed to complement the material-blood interaction.

A degradation test according to ISO 10993-14 will be done to evaluate the degradation of CaP/CNTs composite and CaP matrix, and assess the level of release of CNTs from the composite structure into the medium. This study is important to predict the behaviour of the novel composite once implanted *in vivo* in bone defects.

## References

1. Enderle J, Blanchard S, Bronzino J. Introduction to Biomedical Engineering. Second Edition ed. California: Elsevier Academic Press; 2005.
2. Hench LL. Biomaterials: a forecast for the future. *Biomaterials*. 1998;19:1419-23.
3. Atala A, Lanza R, Thomson J, Nerem R. Foundations of Regenerative Medicine. First edition ed. Lee H, park TG, editors: Elsevier Academic Press; 2010.
4. Kahanovitz N. Electrical stimulation of spinal fusion: a scientific and clinical update. *The spine journal*. 2002;2:145-50.
5. Fernandes MH. Fundamental Aspects of Bone Biology. Porto: Faculdade de Medicina Dentária da Universidade do Porto; 1999. p. 70-84.
6. Robinson R, Watson ML. Collagen-crystal relationships in bone as seen in the electron microscope. *Anatomical Record*. 1952;114:383-410.
7. Kiely C, Hopkinson I, Grant M. Connective Tissue and Its Heritable Disorders: Molecular, Genetic, and Medical Aspects: Wiley-Liss; 1993.
8. Fernandes MH. Mecanismos de Regulação do Metabolismo Ósseo. *Acta Médica Portuguesa*. 1998;11:41-52.
9. Ratner BD, Hoffman AS, Schoen FJ, Lemons JE. Biomaterials Science: An introduction to materials in medicine. California: Academic Press; 1996.
10. Teixeira SMS. Bioactive ceramics with high specific surface area for osteoconduction. Porto: Faculdade de Engenharia da Universidade do Porto; 2008.
11. Seeley RR, Stephens TD, Tate P. Anatomia e Fisiologia. Sixth Edition ed: McGraw-Hill Higher Education 2005.
12. Duncan RL, Turner CH. Mechanotransduction and the functional response of bone to mechanical strain. *Calcified Tissue International*. 1995;57:344-58.
13. Turner CH, Pavalko FM. Mechanotransduction and functional response of the skeleton to physical stress: the mechanisms and mechanics of bone adaptation. *Journal of Orthopaedic Science*. 1998;3:346-55.
14. Woo SL, Kuei SC, Amiel D, Gomez MA, Hayes WC, White FC, et al. The effect of prolonged physical training on the properties of long bone: a study of Wolff's Law. *The Journal of Bone & Joint Surgery*. 1981;63:780-7.
15. Martonosi AN. Animal Electricity.  $\text{Ca}^{2+}$  and muscle contraction. A brief history of muscle research. *Acta Biochim Pol*. 2000;47:493-516.
16. Chao PH, Roy R, Mauck RL, Liu W, Valhmu WB, Hung CT. Chondrocyte translocation response to direct current electric fields: A review. *J Biomech Eng*. 2000;122:261-7.
17. Sierpowska J, Hakulinen MA, Töyräs J, Day JS, Weinans H, Jurvelin JS, et al. Prediction of mechanical properties of human trabecular bone by electrical measurements. *Physiol Meas*. 2005;26:S119-S31.

18. Bennett MI, johnson MI, Brown SR, Radford H, Brown JM, Searle RD. Feasibility study of transcutaneous electrical nerve stimulation (TENS) for cancer bone pain. *The Journal of Pain*. 2010;11(4):351-9.
19. Fleischli JG, laughlin TJ. Electrical Stimulation in Wound Healing. *The Journal of Foot & Ankle Surgery*. 1997;36(6):457-61.
20. Huang CP, Chen XM, Chen ZQ. Osteocyte: the impresario in the electrical stimulation for bone fracture healing medical hypotheses. 2007;70:287-90.
21. Wiesmann H-P, Hartig M, Stratmann U, Meyer U, Joos U. Electrical stimulation influences mineral formation of osteoblast-like cells in vitro. *biochimica et biophysica acta*. 2000;1538:28-37.
22. Yonemori K, Matsunaga S, Ishidou Y, Maeda S, Yoshida H. Early Effects of Electrical Stimulation on Osteogenesis. *Bone* 1996;19(2):173-80.
23. Zizic TM, Hoffman KC, Holt PA, Hungerford DS, O'Dell JR, Jacobs MA, et al. The treatment of osteoarthritis of the knee with pulsed electrical stimulation. *The Journal of Rheumatology*. 1995;22(9):1757-61.
24. Searle RD, Bennett MI, Johson MI, Callin S, Radford H. Transcutaneous electrical nerve stimulation (TENS) for cancer bone pain. *Journal of Pain and Symptom Management*. 2009;37(3):424-8.
25. Figueiredo VS. a referência em Fisioterapia. In: Vitalino Sousa Figueiredo L, editor. Gondomar2009.
26. Mellen CR, inventor Chamberlain, assignee. Electrical stimulation device and methods of treatment of various body conditions. Salt Lake City patent 6735476. 2002.
27. De Long WG, Einhorn TA, Koval K, McKee M, Smith W, Sanders R, et al. Bone Grafts and Bone Graft Substitutes in Orthopaedic Trauma Surgery. A Critical Analysis. *The Journal of Bone and Joint Surgery*. 2007;89(3):649-58.
28. Giannoudis P, Dinopoulos H, Tsiridis E. Bone substitutes: An update. *Injury*. 2005;36(3):S20-S7.
29. Lutolf MP, Weber FE, Schmoekel HG, Schense JC, Kohler T, Müller R, et al. Repair of bone defects using synthetic mimetics of collagenous extracellular matrices. *Nature Biotechnology*. 2003;21:513-8.
30. Nandi SK, Roy S, MUkherjee P, Kundu B, De DK, Basu D. Orthopaedic applications of bone graft & graft substitutes: a review. *Indian J Med Res*. 2010;132:15-30.
31. Parikh SN. Bone graft substitutes in modern orthopedics Orthopedics. 2002;25(11):1301-9.
32. Yoshikawa T. Bone reconstruction by cultured bone graft. *Materials Science and Engineering C - Biomimetic and Supramolecular Systems*. 2000;13(1-2):29-37.
33. Bauer TW. Bone graft materials: an overview of the bascia science. *Clinical Orthopedics and related research*. 2000;371:10-27.
34. Gutierres M, Lopes MA, Hussain NS, Cabral AT, Almeida L, Santos JD. Substitutos Ósseos Conceitos Gerais e Estado Actual. *Arquivos de Medicina*. 2006;19(4):153-62.

35. Fleming JE, Cornell CN, Muschler GE. Bone cells and matrices in orthopedic tissue engineering. *Orthop Clin N Am.* 2000 Jul;31(3):357-+.
36. Muschler GF, Negami S, Hyodo A, Scerbin V, Kambic H. Collagen Ceramic Composites as Graft for Spinal-Fusion. *J Bone Miner Res.* 1995 Aug;10:S306-S.
37. Wahl D, Czernuszka J. Collagen-Hydroxyapatite composites for hard tissue repair. *European Cells and Materials.* 2006;11:43-56.
38. Zabeu JLA, Mercadante M. Bone graft substitutes compared to autologous bone graft in orthopedic surgery – Systematic literature review. *Rev Bras Ortop.* 2008;43(3):59-68.
39. Lopes MA, Knowles JC, Kuru L, Santos JD, Monteiro FJ, Olsen I. Flow cytometry for assessing biocompatibility. *J Biomed Mater Res.* 1998;41(4):649-56.
40. Lopes MA, Knowles JC, Santos JD, Monteiro FJ, Olsen I. Direct and indirect effects of P<sub>2</sub>O<sub>5</sub> glass reinforced-hydroxypatite composites on the growth and function of osteoblast-like cells. *Biomaterials.* 2000;21(11):1165-72.
41. Santos JD, Knowles JC, Reis RL, Monteiro FJ, Hastings GW. Microstructural characterization of glass-reinforced hydroxyapatite composites. *Biomaterials.* 1994;15(1):5-10.
42. Fujimoto M, Isobe M, Yamaguchi S, Amagasa T, Watanabe A, Ooya T, et al. Poly(ethylene glycol) hydrogels cross-linked by hydrolyzable polyrotaxane containing hydroxyapatite particles as scaffolds for bone regeneration. *J Biomat Sci-Polym E.* 2005;16(12):1611-21.
43. Zhou ZY, Ren YJ, Yang DZ, Nie J. Performance improvement of injectable poly(ethylene glycol) dimethacrylate-based hydrogels with finely dispersed hydroxyapatite. *Biomedical Materials.* 2009 Jun;4(3):-.
44. Zhou ZY, Yang DZ, Nie J, Ren YJ, Cui FZ. Injectable Poly(ethylene glycol) Dimethacrylate-based Hydrogels with Hydroxyapatite. *J Bioact Compat Pol.* 2009 Sep;24(5):405-23.
45. Lee SH, Kim BJ, Shin SH, Kim HS, Kim KC, Kim CH, et al. Guided Bone Regeneration Effect by Chitosan/Hydroxyapatite Membrane on Repair of Rat Calvarial Defect. *Tissue Eng Regen Med.* 2009 Jun;6(4-11):916-23.
46. Tachaboonyakiat W, Serizawa T, Akashi M. Hydroxyapatite formation on/in biodegradable chitosan hydrogels by an alternate soaking process. *Polym J.* 2001;33(2):177-81.
47. Wu T, Nan KH, Chen JD, Jin D, Jiang S, Zhao PR, et al. A new bone repair scaffold combined with chitosan/hydroxyapatite and sustained releasing icariin. *Chinese Sci Bull.* 2009 Sep;54(17):2953-61.
48. Yoshida A, Miyazaki T, Ishida E, Ashizuka M. Preparation of bioactive chitosan-hydroxyapatite nanocomposites for bone repair through mechanochemical reaction. *Mater Trans.* 2004 Apr;45(4):994-8.
49. Bernhardt A, Despang F, Lode A, Demmler A, Hanke T, Gelinsky M. Proliferation and osteogenic differentiation of human bone marrow stromal cells on alginate-getatine-hydroxyapatite scaffolds with anisotropic pore structure. *J Tissue Eng Regen M.* 2009 Jan;3(1):54-62.

50. Lin HR, Yeh YJ. Porous alginate/hydroxyapatite composite scaffolds for bone tissue engineering: Preparation, characterization, and in vitro studies. *J Biomed Mater Res B*. 2004 Oct 15;71B(1):52-65.
51. Lu L, Qi YS, Zhou CR, Jiao YP. Rapidly in situ forming biodegradable hydrogels by combining alginate and hydroxyapatite nanocrystal. *Sci China Technol Sc*. 2010 Jan;53(1):272-7.
52. Marsich E, Semeraro S, Turco G, Bellomo F, Donati I, Paoletti S. Porous Nano-Hydroxyapatite/Alginate Scaffolds for Bone Regeneration. *Tissue Eng Pt A*. 2009 May;15(5):O15-O6.
53. Turco G, Marsich E, Bellomo F, Semeraro S, Donati I, Brun F, et al. Alginate/Hydroxyapatite Biocomposite For Bone Ingrowth: A Trabecular Structure With High And Isotropic Connectivity. *Biomacromolecules*. 2009 Jun;10(6):1575-83.
54. Ajayan PM, Stephan O, Colliex C, Trauth D. Aligned Carbon Nanotube Arrays Formed by Cutting a Polymer Resin-Nanotube Composite. *Science*. 1994 Aug 26;265(5176):1212-4.
55. Tanaka K, Yamabe T, Fukui K. The science and technology of carbon nanotubes: Elsevier; 1999.
56. Sahithi K, Swetha M, Ramasamya K, Sriniyan N, Selyamurugan N. Polymeric composites containing carbon nanotubes for bone tissue engineering. *Int J Biol Macromol*. 2010 Apr 1;46(3):281-3.
57. Saito N, Usui Y, Aoki K, Narita N, Shimizu M, hara K, et al. Carbon nanotubes: biomaterial applications. The Royal Society of Chemistry. 2009;38:1897-903.
58. Campidelli S, klumpp C, Bianco A, Guldi DM, Prato M. Functionalization of CNT: Synthesis and applications in photovoltaics and biology. *Journal of Physical Organic Chemistry*. 2006;19:531-9.
59. McClory C, Chin SJ, McNally T. Polymer/Carbon Nanotube Composites. *Aust J Chem*. 2009;62:762-85.
60. Ajayan PM. Nanotubes from carbon. *Chem Rev*. 1999;99:1787-99.
61. Baughman RH, Zakhidov AA, Heer WA. Carbon nanotubes-the route toward applications. *Science*. 2002;297:787-92.
62. Mamalis AG, Votgländer LOG, Markopoulos A. Nanotechnology and nanostructured materials: trends in carbon nanotubes *Precis Eng*. 2004;28:16-30.
63. Endo M, Strano MS, Ajayan PM. Potential applications of carbon nanotubes. *Physics*. 2008;111:13-61.
64. Araújo R, Paiva MC, Proença MF, Silva CJR. Functionalization of carbon nanofibers by 1,3-dipolar cycloaddition reactions and its effect on composite properties. *Composites Science and Techonology*. 2007;67:806-10.
65. Bahr JL, Tour JM. Covalent chemestry of single-wall carbon nanotubes. *J Mater Chem*. 2002;12:1952-8.
66. Tasis D, Tagmatarchis N, Georgakilas V, Prato M. Soluble carbon nanotubes. *Chem Eur J*. 2003;9(4000-4008).

67. Srinivasan C. Toxicity of carbon nanotubes - Some recent studies. *Current Science*. 2008;95(3).
68. Tsotra P, Friedrich K. Electrical and mechanical properties of functionally graded epoxy-resin/carbon fibre composites. *Composites*. 2003;34:75-82.
69. Lewinski N, Colvin V, Drezek R. Cytotoxicity of Nanoparticles. *Small*. 2008;4(1):26-49.
70. Höck J, editor. Proceedings of the workshop on research projects on the safety of nanomaterials: reviewing the knowledge gaps. Workshop proceedings; 2008; Brussels.
71. Pagona G, Tagmatarchis N. Carbon Nanotubes: Materials for Medicinal Chemistry and Biotechnological Applications. *Current Medicinal Chemistry*. 2006;13:1789-98.
72. Zawadzak E, Bil M, Ryszkowska J, Nazhat SN, Cho J, Bretcanu O, et al. Polyurethane foams electrophoretically coated with carbon nanotubes for tissue engineering. *Biomedical Materials*. 2009;4.
73. Supronowicz PR, Ajayan PM, Ullmann KR, Arulanandam BP, Metzger DW, Bizios R. Novel current-conducting composite substrates for exposing osteoblasts to alternating current stimulation. *J Biomed Mater Res*. 2002 Mar 5;59(3):499-506.
74. Supronowicz PR, Ullmann KR, Ajayan PM, Arulanandam BP, Metzger DW, Bizios R. Electrical stimulation enhances cellular/molecular functions of osteoblasts relevant to new bone formation in vitro. *P Ann Int Ieee Embs*. 2001;23:2979-80  
4132.
75. Armentano I, Marinucci L, Dottori M, Balloni S, Fortunati E, Pennacchi M, et al. Novel poly(L-lactide) PLLA/SWNTs nanocomposites for biomedical applications: material characterization and biocompatibility evaluation. *J Biomater Sci Polym Ed*. 2011;22(4-6):541-56.
76. Reis J, Kanagaraj S, Fonseca A, Mathew MT, Capela-Silva F, Potes J, et al. In vitro studies of multiwalled carbon nanotube/ultrahigh molecular weight polyethylene nanocomposites with osteoblast-like MG63 cells. *Braz J Med Biol Res*. 2010 May;43(5):476-82.
77. Zawadzak E, Bil M, Ryszkowska J, Nazhat SN, Cho J, Bretcanu O, et al. Polyurethane foams electrophoretically coated with carbon nanotubes for tissue engineering scaffolds. *Biomed Mater*. 2009 Feb;4(1):015008.
78. Sitharaman B, Shi X, Walboomers XF, Liao H, Cuijpers V, Wilson LJ, et al. In vivo biocompatibility of ultra-short single-walled carbon nanotube/biodegradable polymer nanocomposites for bone tissue engineering. *Bone*. 2008 Aug;43(2):362-70.
79. Aryal S, Bahadur KCR, Dharmaraj N, Kim K-W, Kim HY. Synthesis and characterization of hydroxyapatite using carbon nanotubes as a nano-matrix. *Scripta Materialia*. 2006;54:131-5.
80. Tan Q, Zhang K, Gu S, Ren J. Mineralization of surfactant functionalized multi-walled carbon nanotubes (MWNTs) to prepare hydroxyapatite/MWNTs nanohybrid. *Applied Surface Science*. 2009;255:7036-9.

81. Tanaka M-a, Onoki T, Omori M, Okubo A, Hashida T. Mechanical Properties of Carbon Nanotubes/Composites prepared by spark plasma sintering. In: Tokuyama M, Maruyama S, editors. Flow Dynamics, The Second International Conference on Flow Dynamics: American Instituto of Physics; 2006. p. 430-2.
82. Li A, Sun K, Dong W, Zhao D. Mechanical properties, microstruture and histocompatibility of MWCNTs/HAp biocomposites. Materials Letters. 2007;61:1839-44.
83. Xu JL, Khor KA, Sui JJ, Chen WN. Preparation and characterization of a novel hydroxyapatite/carbon nanotubes composite and its interaction with osteoblast-like cells. Materials Science and Engineering C. 2009;29:44-9.
84. Lahiri D, Benaduce AP, Rouzaud F, Solomon J, Keshri AK, Kos L, et al. Wear behavior and in vitro cytotoxicity of wear debris generated from hydroxyapatite-carbon nanotube composite coating. J Biomed Mater Res A. 2011 Jan;96(1):1-12.
85. Hahn B, Lee J, Park D, Choi J, Ryu J, Yoon W, et al. Mechanical and in vitro biological performances of hydroxyapatite-carbon nanotube composite coatings deposited on Ti by aerosol deposition. Acta Biomater. 2009;5:3205-14.
86. Wu MX, Gordon RE, Herbert R, Padilla M, Moline J, Mendelson D, et al. Case Report: Lung Disease in World Trade Center Responders Exposed to Dust and Smoke: Carbon Nanotubes Found in the Lungs of World Trade Center Patients and Dust Samples. Environ Health Persp. 2010 Apr;118(4):499-504.
87. Balani K, Anderson R, Laha T, Andara M, Tercero J, Crumpler E, et al. Plasma-sprayed carbon nanotube reinforced hydroxyapatite coatings and their interaction with human osteoblasts in vitro. Biomaterials. 2007;28:618-24.
88. Tan Q, Zhang K, Gu S, Ren J. Mineralization of surfactant functionalized multi-walled carbon nanotubes (MWNTs) to prepare hydroxyapatite/MWNTs nanohybrid. Applied Surface Science. 2009;255(15):7036-9.
89. Andrada D, Vieira HS, Mendonça Rd, Santos AP, Martins MD, Macedo WAA, et al. Estudod e nanotubes de carbono modificados quimicamente por espectroscopia de fotoelétrons excitados por raios-x. 29º Encontro Regional da Sociedade Brasileira de Química - MG; Águas de Lindoia2006.
90. Proença MF, Araujo RF, Paiva MC, Silva CJR. The Diels-Alder Cycloaddition Reaction in the Functionalization of Carbon Nanofibers. J Nanosci Nanotechno. 2009 Oct;9(10):6234-8.
91. Chang Y.H F, Li H. and Rong B.Z. A study concerning the pretreatment of CNTs and its influence on the performance of NiB/CNTs amorphous catalyst. J Serb Chem Soc. 2006;71(11):1153–60.
92. White AA. Production and characterisation of hydroxyapatite/multi-walled carbon nanotube composites. Cambridge: University of Cambridge; 2009.
93. da Silva MHP, Lemos AF, Ferreira JMF, Lopes MA, Santos JD. Production of porous biomaterials based on glass-reinforced hydroxyapatite composites. Advanced Materials Forum I. 2002;230-2:483-6.

94. M. A. Lopes FJM, J. D. Santos, A. P. Serro, B. Saramago. Hydrophobicity, surface tension, and zeta potential measurements of glass-reinforced hydroxyapatite composites. *J Biomed Mater Res.* 1999;45:370-5.
95. Deligianni K, Koutsoukos, Missirlis. Effect of surface roughness of hydroxyapatite on human bone marrow cell adhesion, proliferation, differentiation and detachment strength. *Biomaterials.* 2001;22:87-96.
96. Hahn B-D, Park D-S, Choi J-J, Ryu J, Yoon W-H, Choi J-H, et al. Preparation and in vitro characterization of aerosol-deposited hydroxyapatite coatings with different surface roughnesses. *Applied Surface Science.* 2011;257(17):7792-9.
97. Balani K. CY, Harimkar S., Dahotre N.B., Agarwal A. Tribological behavior of plasma-sprayed carbon nanotube-reinforced hydroxyapatite coating in physiological solution. *Acta Biomater.* 2007;3:944-51.
98. Kharitonov RLPaFY. Some Features of the behavior of pure during hot pressing oxides. Plekhanov National Economics Institute and the State Electroceramics Research Institute - Ogneupory. 1966;2:38-42.
99. M.T. Hernandez MG, A. De Pablos. C-diffusion during hot press in the  $\text{Al}_2\text{O}_3$ - $\text{Cr}_2\text{O}_3$  system. *Acta Materialia.* 2003;51:217-28.
100. Wongwitwichot P. KJ, Chua K.H., Ruszymah B.H.I. Comparison of TCP and TCP/HA Hybrid Scaffolds for Osteoconductive Activity The Open Biomedical Engineering Journal. 2010;4:279-85.
101. Kakade B.A. PVK. Tuning the Wetting Properties of Multiwalled Carbon Nanotubes by Surface Functionalization. *J Phys Chem C.* 2008;112(9):3183-6.
102. Pavese M. MS, Bianco S., Giorcelli M, Pugno N. An analysis of carbon nanotube structure wettability before and after oxidation treatment. *JPhys:CondensMatter* 2008;20:474-206.
103. Sun J. GL. Development of a dispersion process for carbon nanotubes in ceramic matrix by heterocoagulation. *Carbon.* 2003;41:1063-8.
104. Chen L. XH, Li Y., Yu W. Surface chemical modification of multiwalled carbon nanotubes by a wet-mechanochemical reaction. *Journal of Nanomaterials.* 2008.
105. Cunha I. Desenvolvimento de substituto ósseo injectável para regeneração óssea. Porto: Faculdade de Engenharia da Universidade do Porto; 2009.
106. Zhao M.L. LDJ, Yuan L., Yue Y.C., Liu H., Sun X. . Differences in cytocompatibility and hemocompatibility between carbon nanotubes and nitrogen-doped carbon nanotubes. *carbon.* 2011;49:3125-33.
107. Narayan R.J. WW, Jin C., Andara M., Agarwal A., Gerhardt R.A., Chun-Che Shih, Chun-Ming Shih, Shing-Jong Lin, Yea-Yang Su, Ramamurti R., Singh R.N. Microstructural and biological properties of nanocrystalline diamond coatings. *Diamond & Related Materials.* 2006;15:1935-40.
108. Henkelman S. RG, Blanton J., Oeveren W. Standardization of incubation conditions for hemolysis testing of biomaterials. *Materials Science and Engineering C* 2009;29:1650-4.

109. Woppard K.J. SS, Chin-Dusting J., Salem H.H., Jackson S.P. Erythrocyte Hemolysis and Hemoglobin Oxidation Promote Ferric Chloride-induced Vascular Injury. *The Journal of Biological Chemistry.* 2009;284(19):13110-8.
110. Yamada S. *Microbiology Lab Diagnostic Flowcharts.* 1998.
111. Rodil SE, Olivar R, Arzate H, Muhl S. Properties of carbon films and their biocompatibility using in-vitro tests. *Diamond & Related Materials.* 2003;12:931-7.
112. Smart SK, Cassady AI, Lu GQ, D.J. M. The biocompatibility of carbon nanotubes. *Carbon.* 2006;44:1034-47.
113. Suia J-L, Lia M-S, Lu Y-P, Yina L-W, Songc Y-J. Plasma-sprayed hydroxyapatite coatings on carbon/carbon composites. *Surface and Coatings Technology.* 2004;176:188-92.
114. Nakanishi K, Sakiyama T, Imamura K. On the Adsorption of Proteins on Solid Surfaces, a Common but Very Complicated Phenomenon *Journal of bioscience and bioengineering.* 2001;91(3):233-44.
115. Araujo JC, Térán FC, Oliveira RA, Nour EAA, Montenegro MAP, Campos JR, et al. Comparison of hexamethyldisilazane and critical point drying treatments for SEM analysis of anaerobic biofilms and granular sludge. *Journal of Electron Microscopy.* 2003;52(4):429-33.
116. Braet F, Zanger Rd, Wisse E. Drying cells for SEM, AFM and TEM by hexamethyldisilazane: a study on hepatic endothelial cells. *Journal of Microscopy.* 1997;186(1):84-7.
117. Oshel P. HMDS and Specimen Drying for SEM. *Microscopy today.* 1997;97(4):16.